MISR overview and observational principles
Data products
Example data applications

David J. Diner
Jet Propulsion Laboratory, California Institute of Technology

Exploring and Using MISR Data
Sydney, Australia
March 2006

MISR characteristics

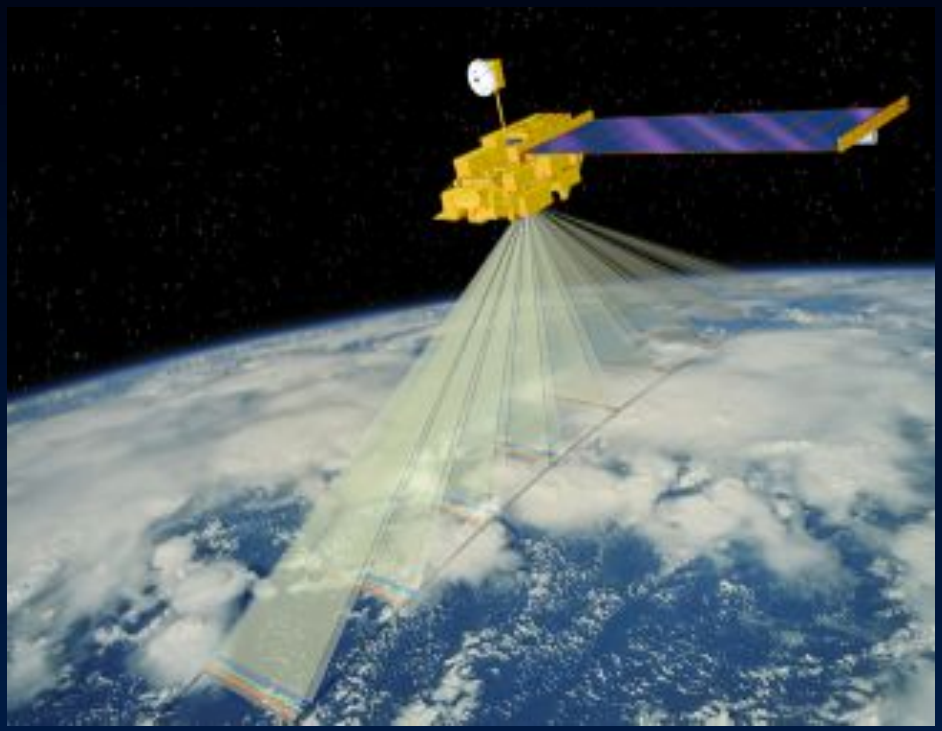

Flies on Terra

9 view angles at Earth surface:
70.5°. 60.0°, 45.6°, 26.1° forward of nadir
nadir
26.1°, 45.6°, 60.0°, 70.5° backward of nadir

Four spectral bands at each angle:
446 nm ± 21 nm
558 nm ± 15 nm
672 nm ± 11 nm
866 nm ± 20 nm

Global Mode (continuous):
275 m sampling in all nadir bands and red band of off-nadir cameras
1.1 km for the other channels

Local Mode (targeted): 275 m all channels

400-km swath: Complete zonal coverage
9 days at equator, 2 days at poles

14-bit quantization

Radiometrically, geometrically calibrated

AirMISR

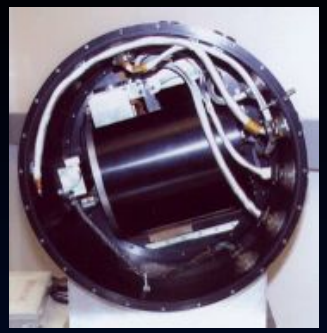

Mounted in nose of NASA ER-2

Covers MISR's nine angles

Uses gimballed MISR prototype camera

27.5 m georectified spatial resolution

9 x 11 km area covered at all angles

Data available at LaRC DAAC

46° images near Howland, ME 28 August 2003

Why multi-angle?

1. Change in reflectance with angle distinguishes different types of aerosols, and surface textures

2. Oblique slant paths through the atmosphere enhance sensitivity to aerosols and thin cirrus

3. Stereo imaging provides geometric heights of clouds and aerosol plumes

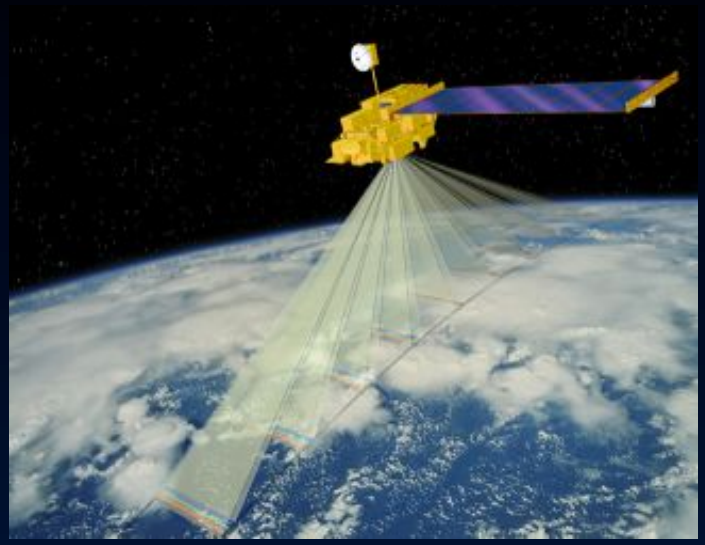

4. Time lapse from forward to backward views makes it possible to use clouds as tracers of winds aloft

5. Different angles of view enable sunglint avoidance or accentuation

6. Integration over angle is required to estimate hemispherical reflectance (albedo) accurately

MISR calibration

Absolute radiometric uncertainty 3%
Relative radiometric uncertainty 2%
Temporal stability 1%
Geolocation uncertainty 50 m
Camera-to-camera registration < 275 m

MISR On-Board Calibrator

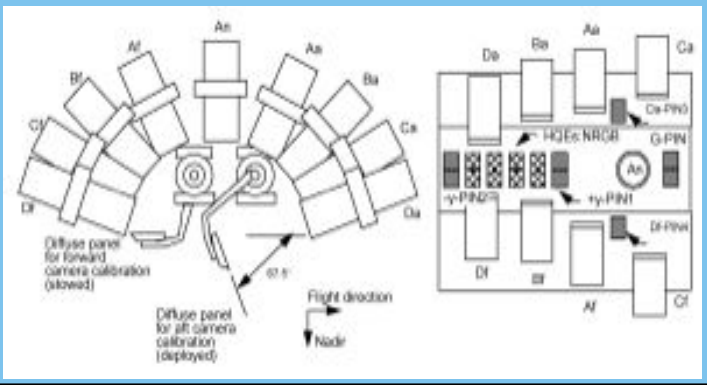

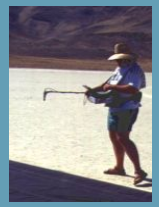

Vicarious calibrations and validations over desert playas and dark water sites

AirMISR

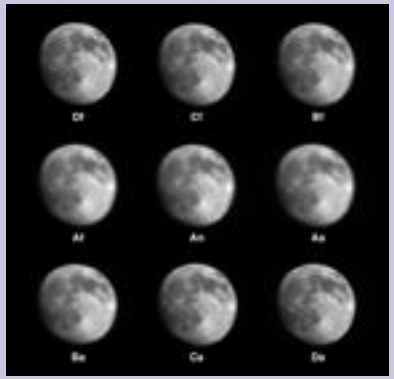

MISR lunar images

MISR geolocation and angle-to-angle coregistration

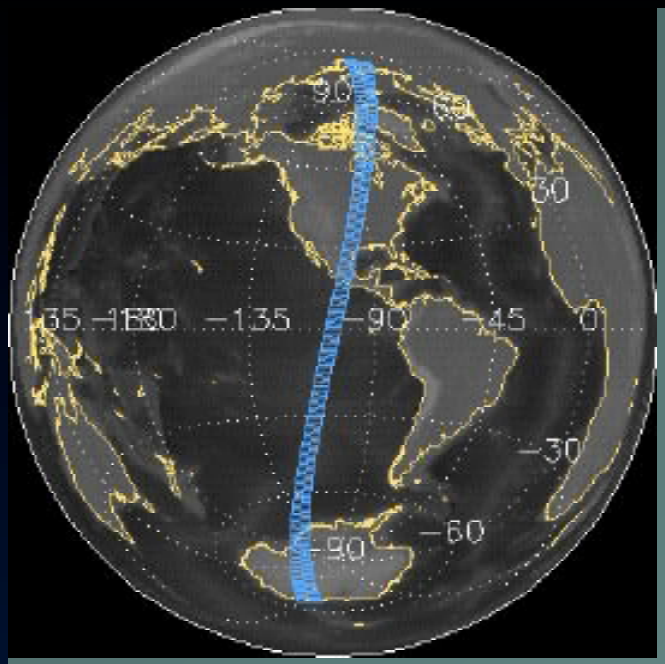

Space Oblique Mercator projection minimizes resampling distortions

233 unique paths in 16-day repeat-cycle of Terra orbit

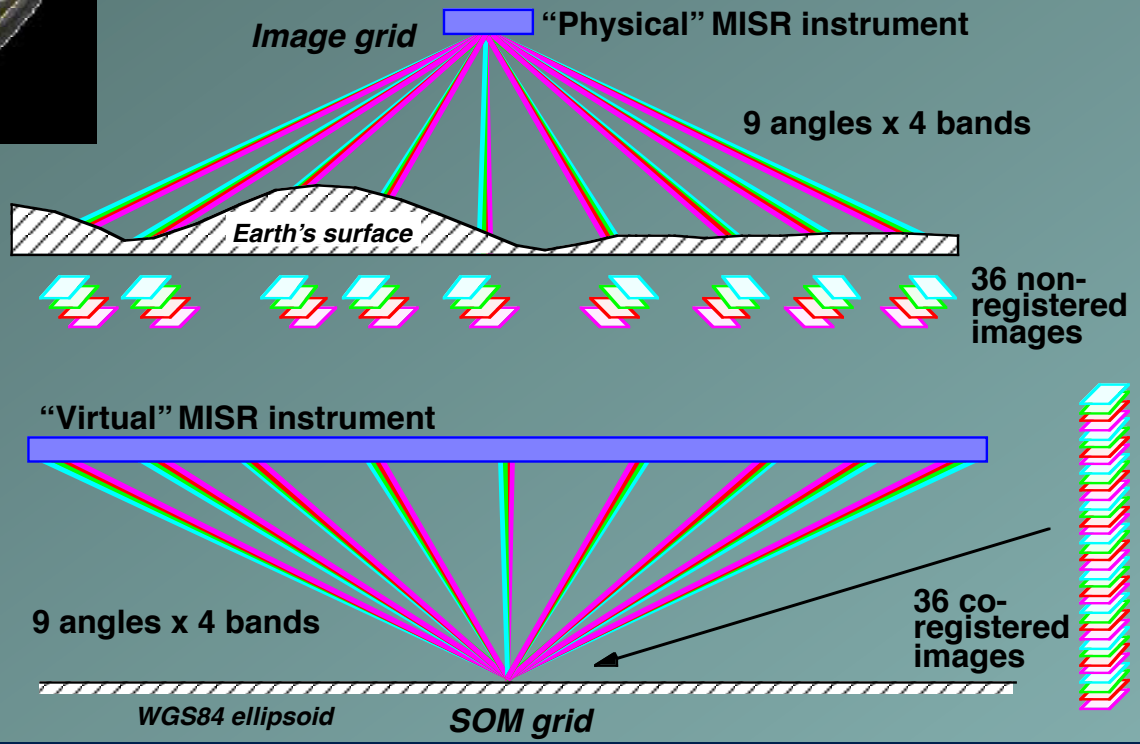

Objects along a camera line-of-sight have multiple “locations” on the Space Oblique Mercator grid

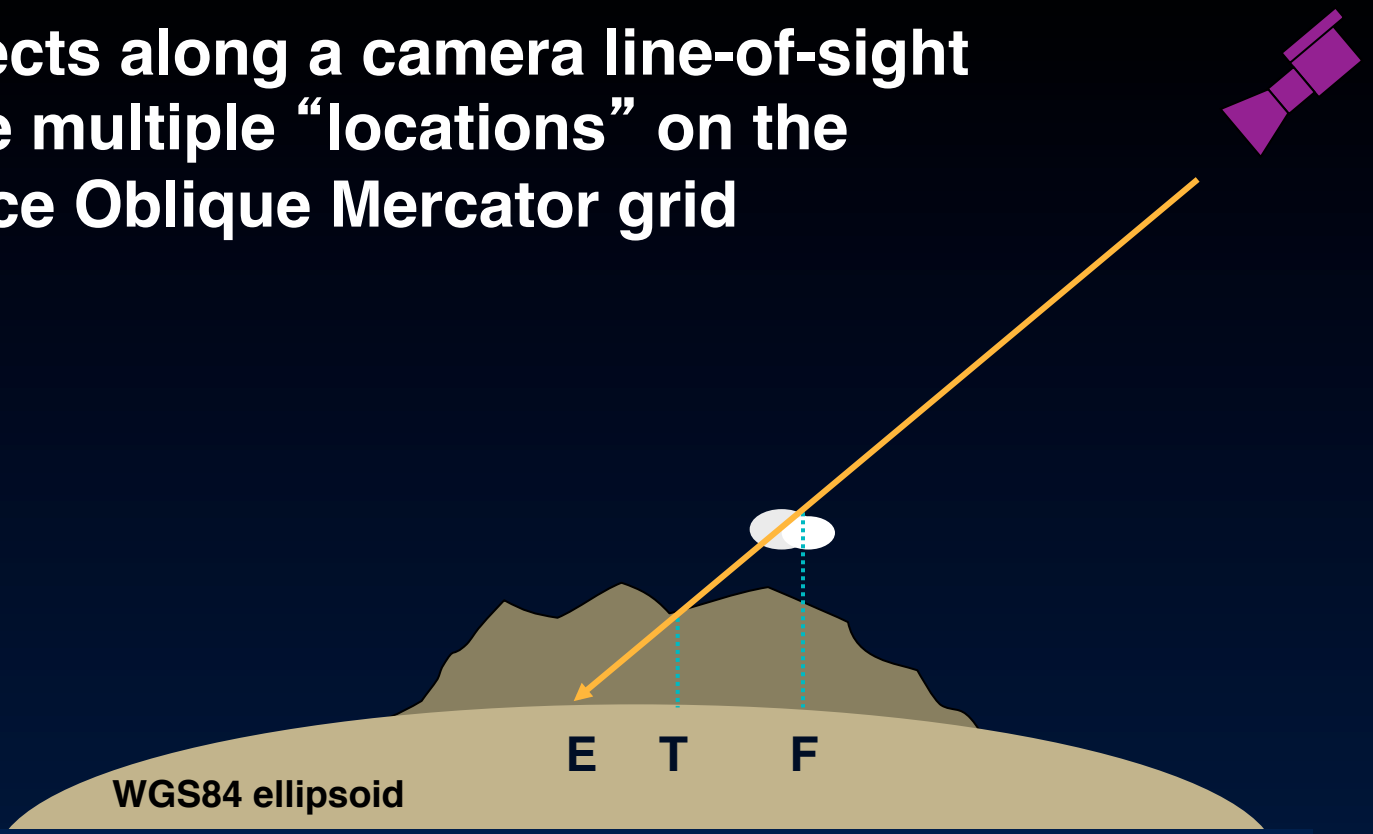

E = ellipsoid-projected location
T = terrain-projected location
F = feature-projected location

Camera-to-camera co-registration requires establishing a reference altitude

"Ellipsoid projection" is to the WGS84 ellipsoid
- performed during Level 1 processing
- used as input to stereoscopic processing

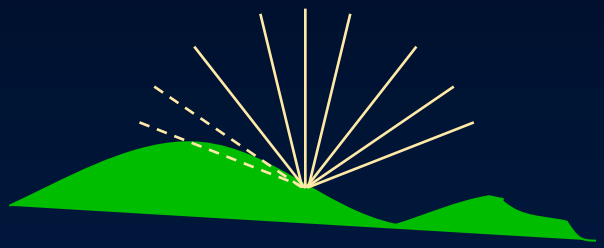

"Terrain projection " is to a digital elevation model
- performed during Level 1 processing
- used as input to aerosol/surface processing
- some views may be obscured

"Feature projection" uses stereoscopically derived cloud heights
- performed during Level 2 processing
- used as input to albedo and cloud classifiers processing

MISR science operations

Global Mode

- Pole-to-pole coverage on orbit dayside
- Full resolution in all 4 nadir bands, and red band of off-nadir cameras (275-m sampling)
- 4x4 pixel averaging in all other channels (1.1-km sampling)

Local Lode

- Implemented for pre-established targets (1-2 per day)
- Provides full resolution in all 36 channels (275-m sampling)
- Pixel averaging is inhibited sequentially from camera Df to camera Da over targets approximately 300 km in length

Calibration

- Implemented bi-monthly
- Spectralon solar diffuser panels are deployed near poles and observed by cameras and a set of stable photodiodes

Level 1 Standard Products

Level 1 standard products

- Level 1A reformatted, annotated product
- Level 1B1 radiometric product
- Level 1B2 georectified radiance product, global and local modes:
  - ellipsoid projected
  - terrain (blocks containing land only) projected
- Level 1B2 browse (JPEG)
- Level 1B2 geometric parameters
- Level 1B2 radiometric camera-by-camera cloud mask

Level 1 processing operates on each camera individually

L1B2 Georectified Radiance Product (MIS03)

Georectified (Earth-projected) radiance data

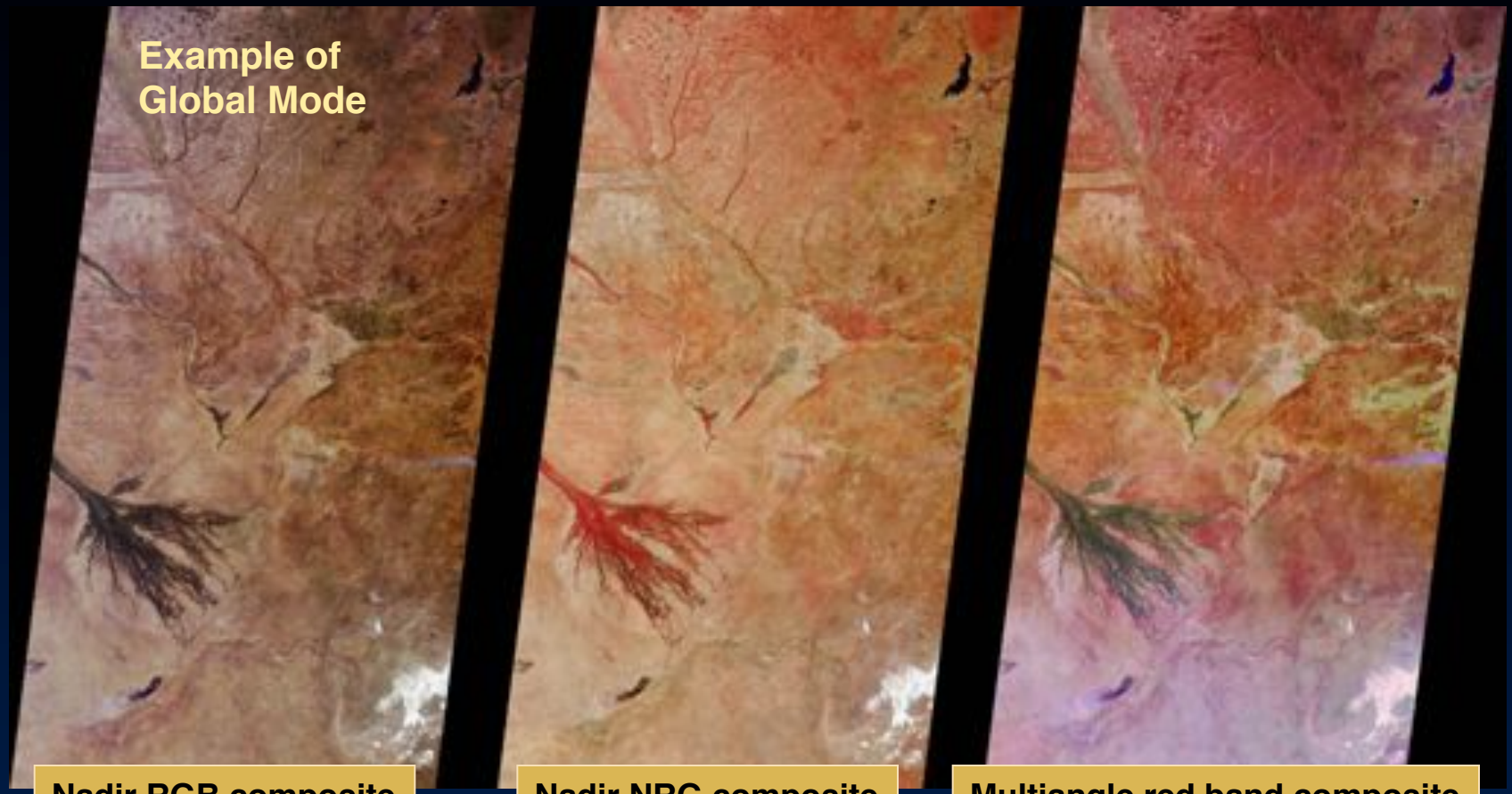

Nadir RGB composite | Nadir NRG composite | Multiangle red band composite

CONTENTS

- Space-Oblique Mercator map-projected calibrated radiances and radiometric data quality indicators (RDQI)
- Scale factors to convert radiances to top-of-atmosphere BRF's

Example of Local Mode

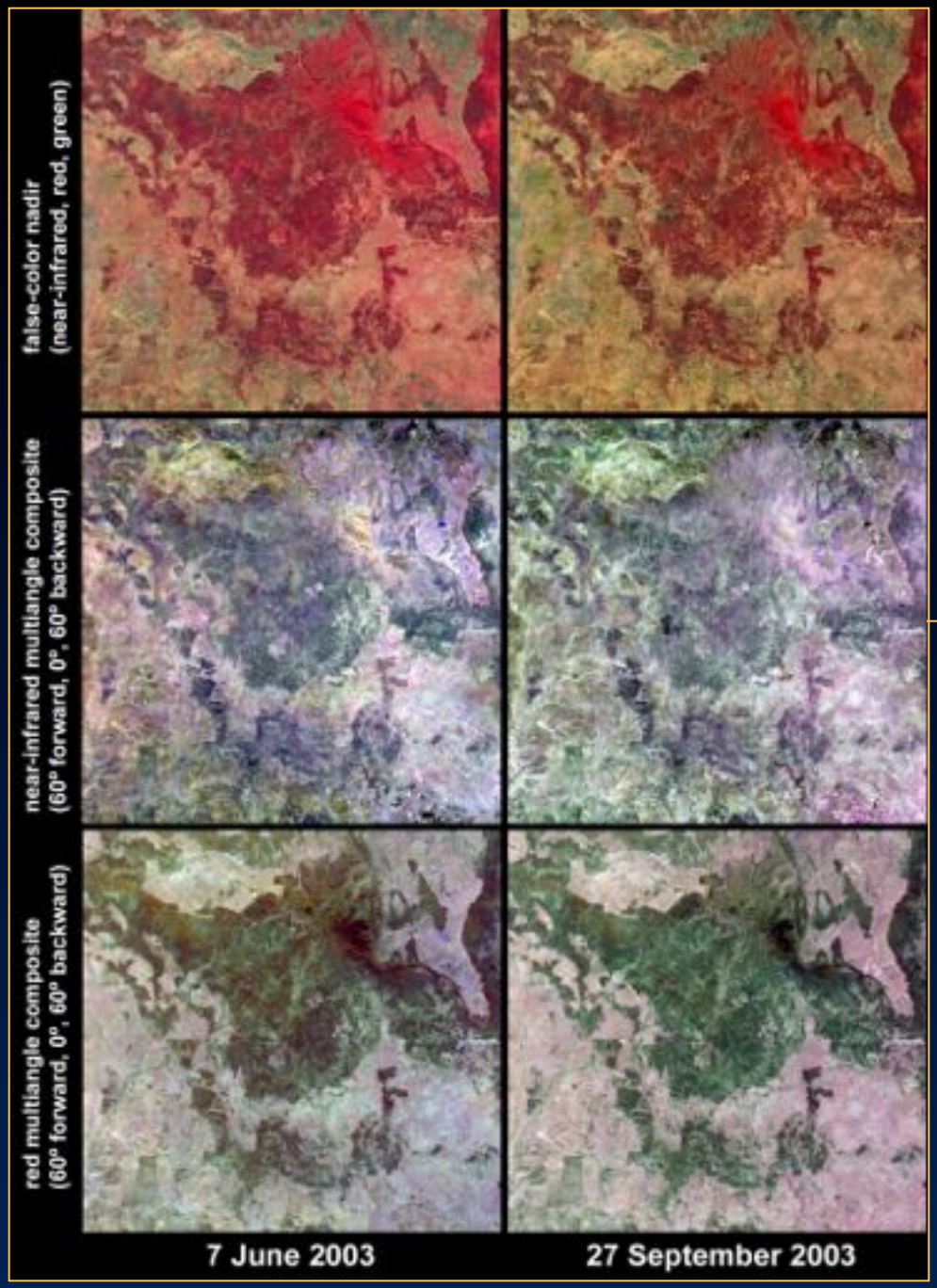

Jet Propulsion Laboratory
California Institute of Technology

MISR
Multi-angle Imaging SpectroRadiometer

HOME | MISSION | GALLERY | EDUCATION | NEWS | ABOUT US | INTERNAL

- Introduction
- EOS and Terra
- MISR Instrument
- Air MISR
- Calibration
- Validation
- Data Products
  - The MISR data system
  - Access data
  - Local Mode data
  - Product maturity levels
- Publications
- FAQ's

Local Mode Data

Contents:

1. Introduction to Local Mode
2. The Local Mode site database
3. Monthly Local Mode data acquisitions
4. Adding new sites
5. Date versus path and orbit (tables)

MISR Local Mode Data Acquisition Database

Short Name	Type	ID	Lat., deg	Long., deg	Elev., m	Campaign	Network
Cairo	OFF	MISR_032	30.05	31.25	170		
Calcutta	OFF	MISR_033	22.5	88.33	0		
Campo_Grand	OFF	MISR_034	-20.43	-54.62	500		Aeronet
Campo_Verde	OFF	MISR_035	-15.6	-55.2	697		Aeronet
Canopy_Crane	OFF	MISR_036	45.82	-122	355		
Carloforte	OFF	MISR_037	8.2	39.1	2286		Aeronet
Camarvon	CAM	MISR_223	-25.5	147.5	400		
CARTEL	OFF	MISR_038	45.4	-71.9	300		Aeronet
Cascades	OFF	MISR_201	44.65	-121.59	1000		
Caspian_Sea	OFF	MISR_039	46	53	0		
Cerrado	OFF	MISR_031	-15.56	-47.53	1047		
Cheju_Is	CAM	MISR_209	33.4	126.5	0.	Ace-Asia	Ace_Asia
Chesapeake	NET	MISR_040	36.9	-75.71	0		CERES
Chicago_Gary	OFF	MISR_041	41.85	-87.65	170		
Chilbolton	OFF	MISR_042	51.14	-1.44	76		
Chobela	OFF	MISR_044	-26.3	32.18	355	Safari	
Chunga	OFF	MISR_045	-15	25.6	1098	Safari	
Churchill	OFF	MISR_046	58.725	-94.12	100		
CLARE_Pature	CAM	MISR_077	-10.767	-62.367	100	CLAIRE 2002	Aeronet
Cont_Shelf	CAM	MISR_226	43.0	-65.0	0.	NewEngland	
Crawford_Pt	OFF	MISR_048	69.88	-46.98	2019		
CRYSTAL_Est	CAM	MISR_211	25.	-79.	0.	CRYSTAL-FACE	
CRYSTAL_Wst	CAM	MISR_212	25.	-82.	0.	CRYSTAL-FACE	
Dakar	OFF	MISR_049	14.4	-17	0		Aeronet
Dalanzadgad	OFF	MISR_050	43.6	104.4	1470		Aeronet
Denver	OFF	MISR_051	39.73	-105	1658		
DYE_2	OFF	MISR_052	66.48	-46.28	2225		GCN
E_Barbuda_Is	CAM	MISR_245	17.63	-60.33	0.	RICO	
EastGulfOman	CAM	MISR_242	23.5	61.0	0	UAE	
Edwards_TX	OFF	MISR_053	33.82	-98.02	268		
Egypt_1	CAL	MISR_204	27.12	26.10	340		
Egypt_Desert	QTR	MISR_054	22.5	28.75	244		
El_Refugio	OFF	MISR_055	-14.8	-60.6	225		Aeronet
EMATREF	OFF	MISR_056	43.916	-1	221		
Eridu	SCI	MISR_247	30.50	46.0			
ETH_CU_Cam	OFF	MISR_057	69.57	-49.3	1356		GCN
Etosha	CAM	MISR_058	-18	17	1129	Safari	
Evora	CAM	MISR_255	38.6	-7.9		SAMUM	
Finland_S	CAM	MISR_216	60.25	24.50	0.		

www-misr.jpl.nasa.gov/mission/data.localmode.html

Changes in scene brightness with angle

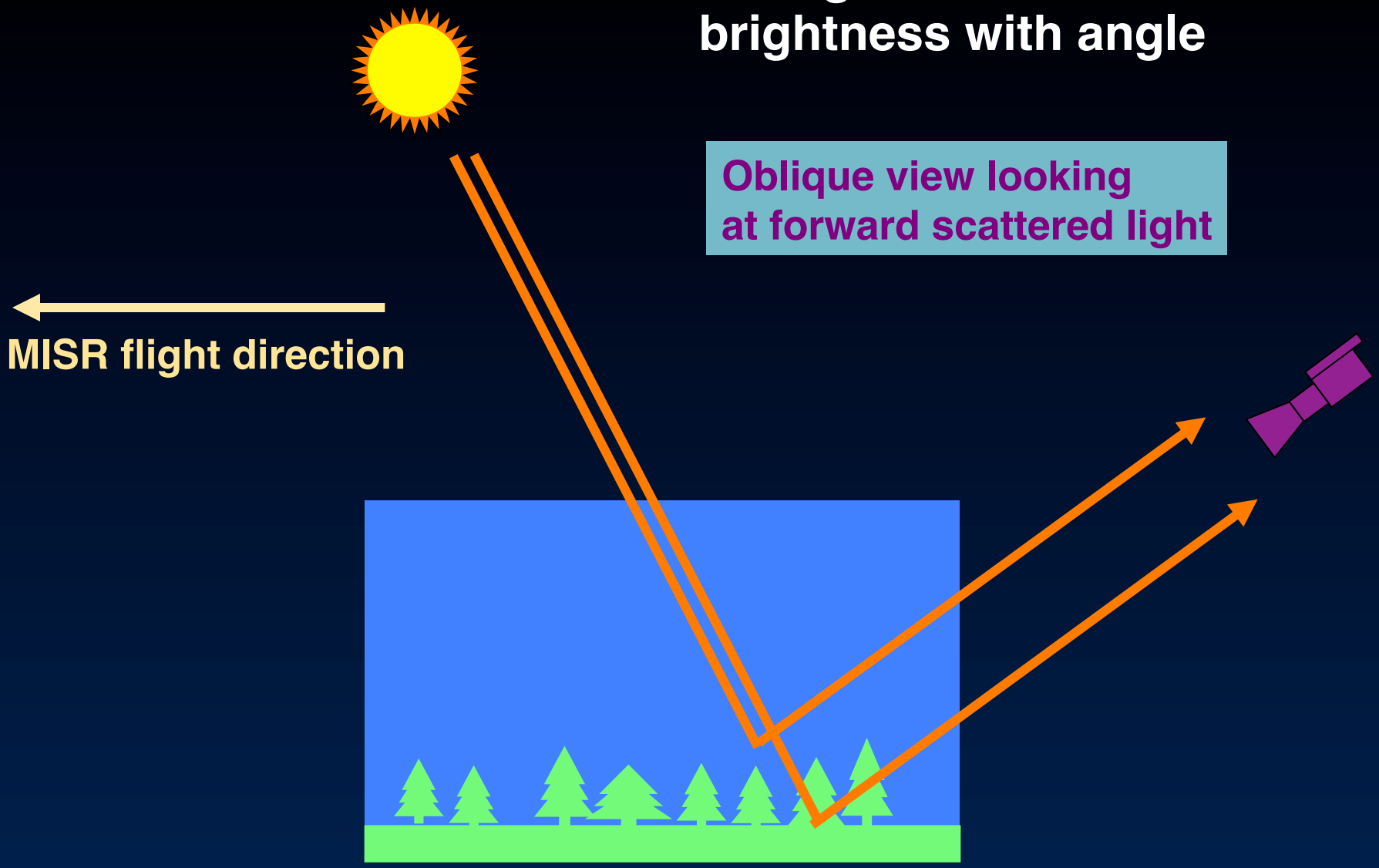

Changes in scene brightness with angle

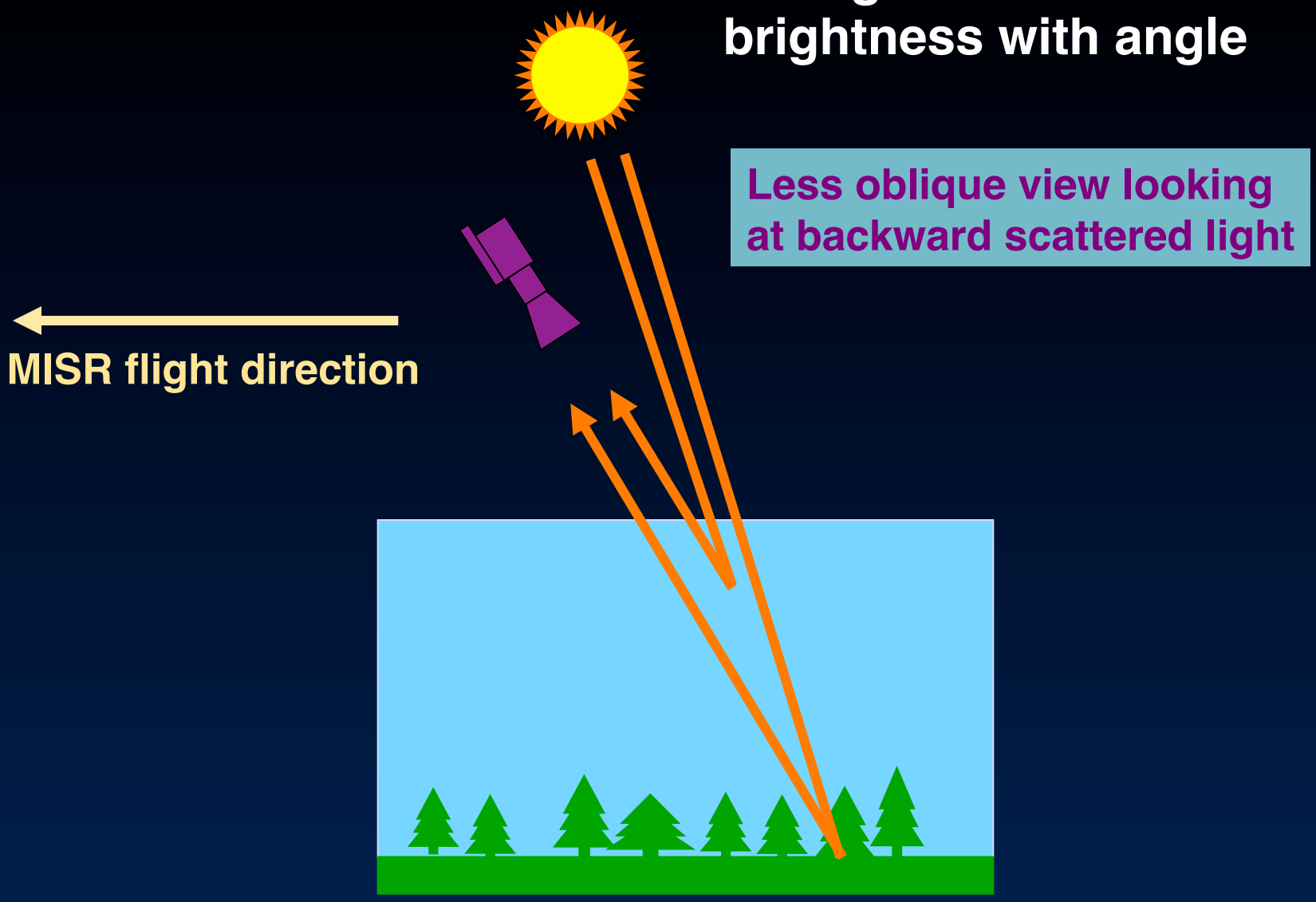

Visualizing surface texture

multi-spectral compositing

Hudson and James Bays
24 February 2000

nadir blue band

nadir green band

nadir red band

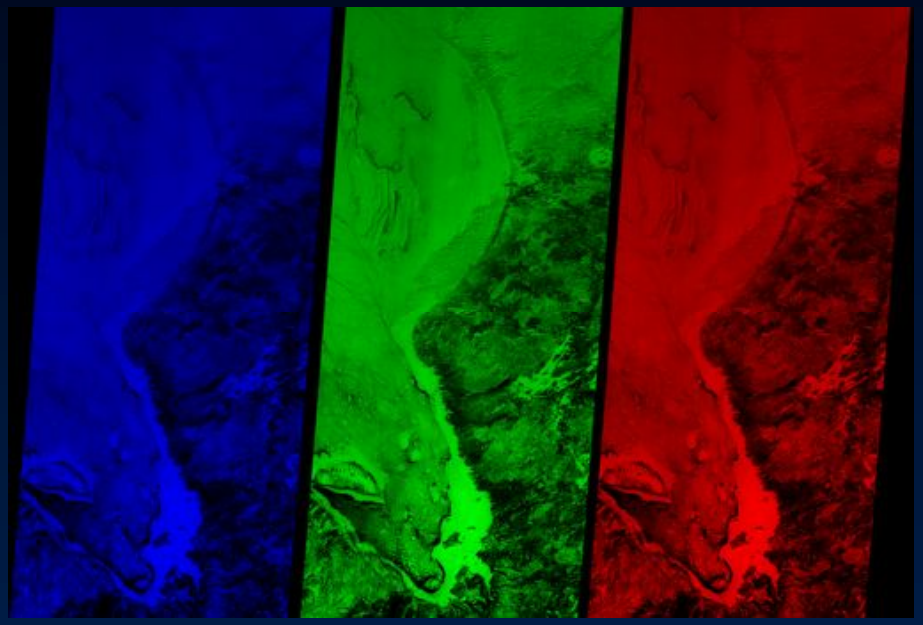

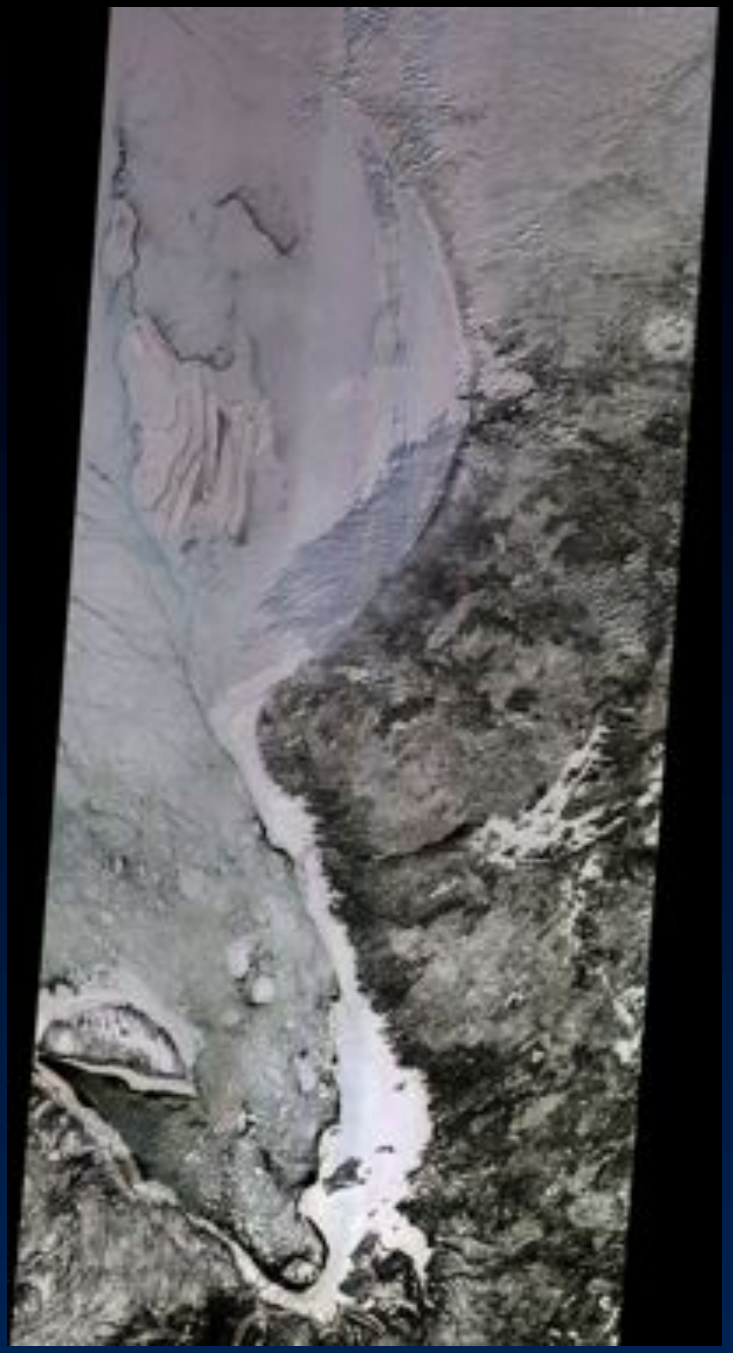

Visualizing surface texture

multi-angle compositing

Hudson and James Bays
24 February 2000

70° forward red band | nadir red band | 70° backward red band

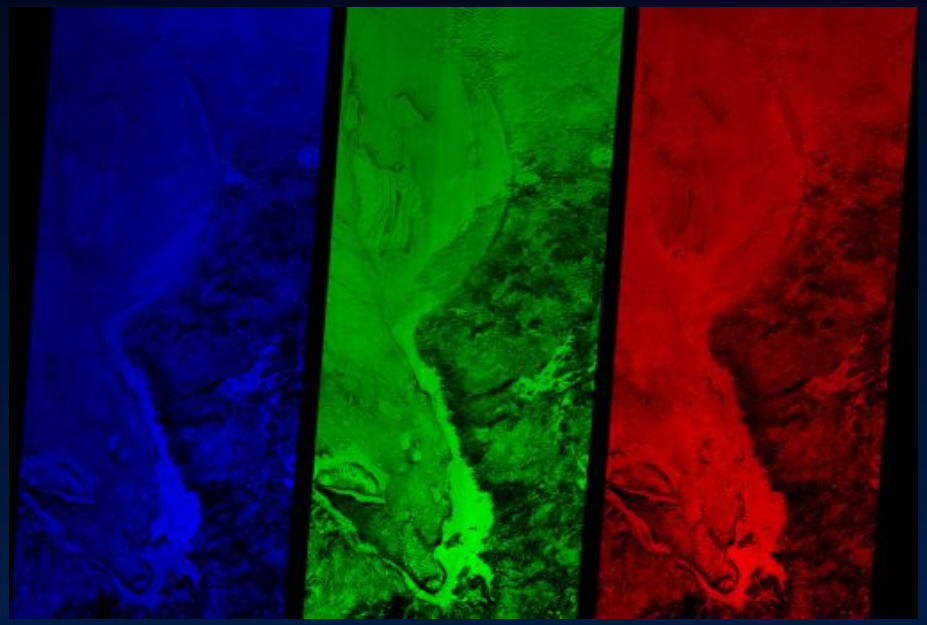

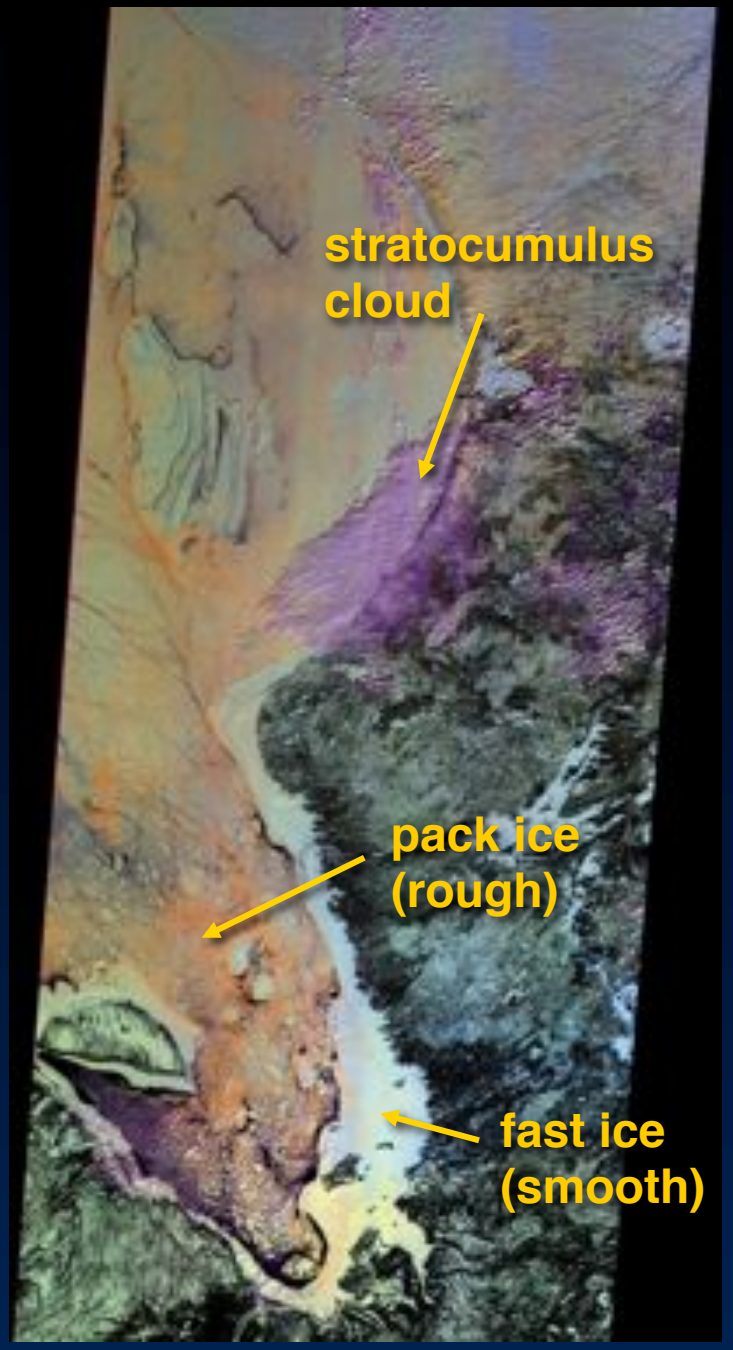

Cloud and ice bidirectional reflectances

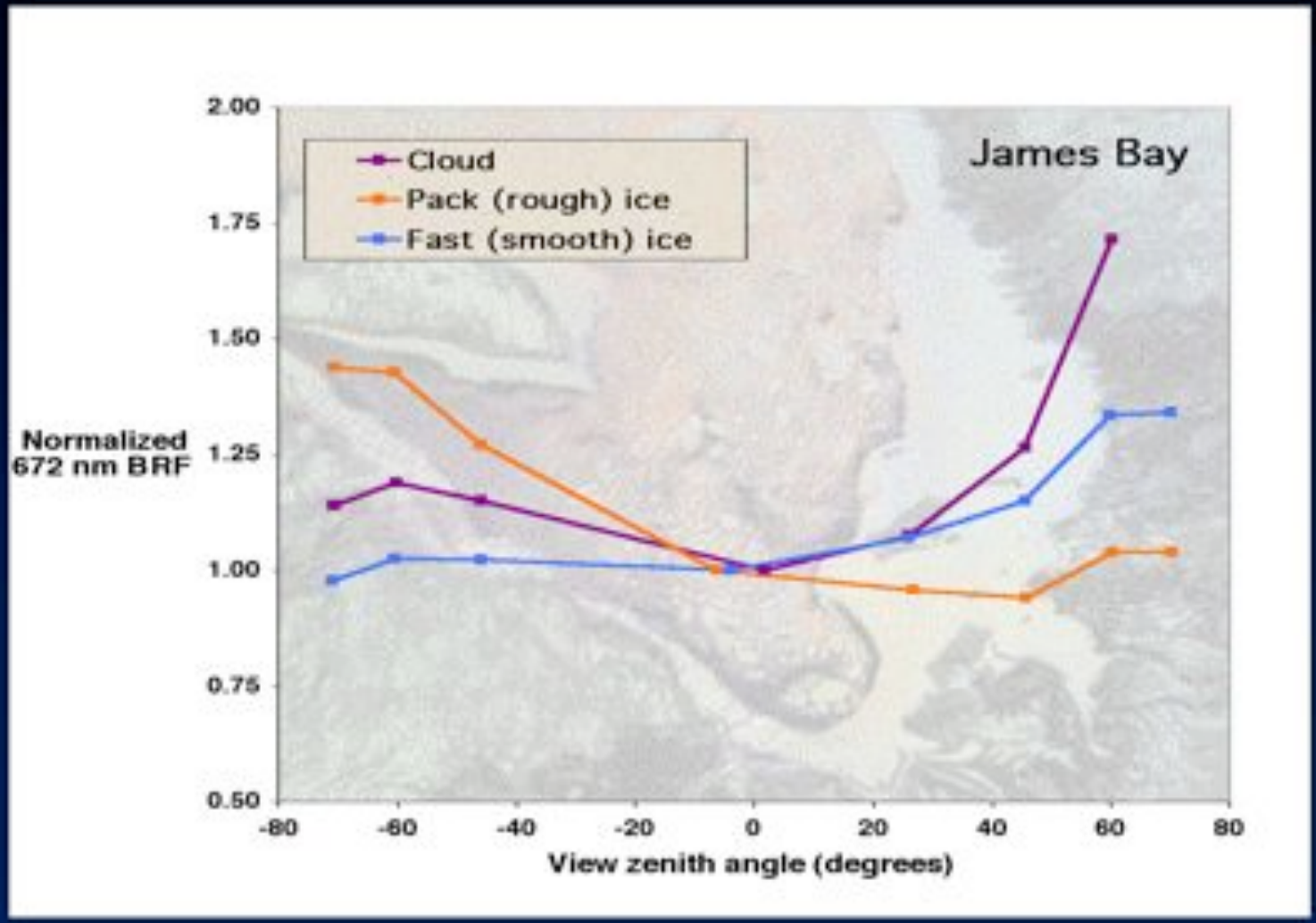

Changes in ice sheet surface roughness

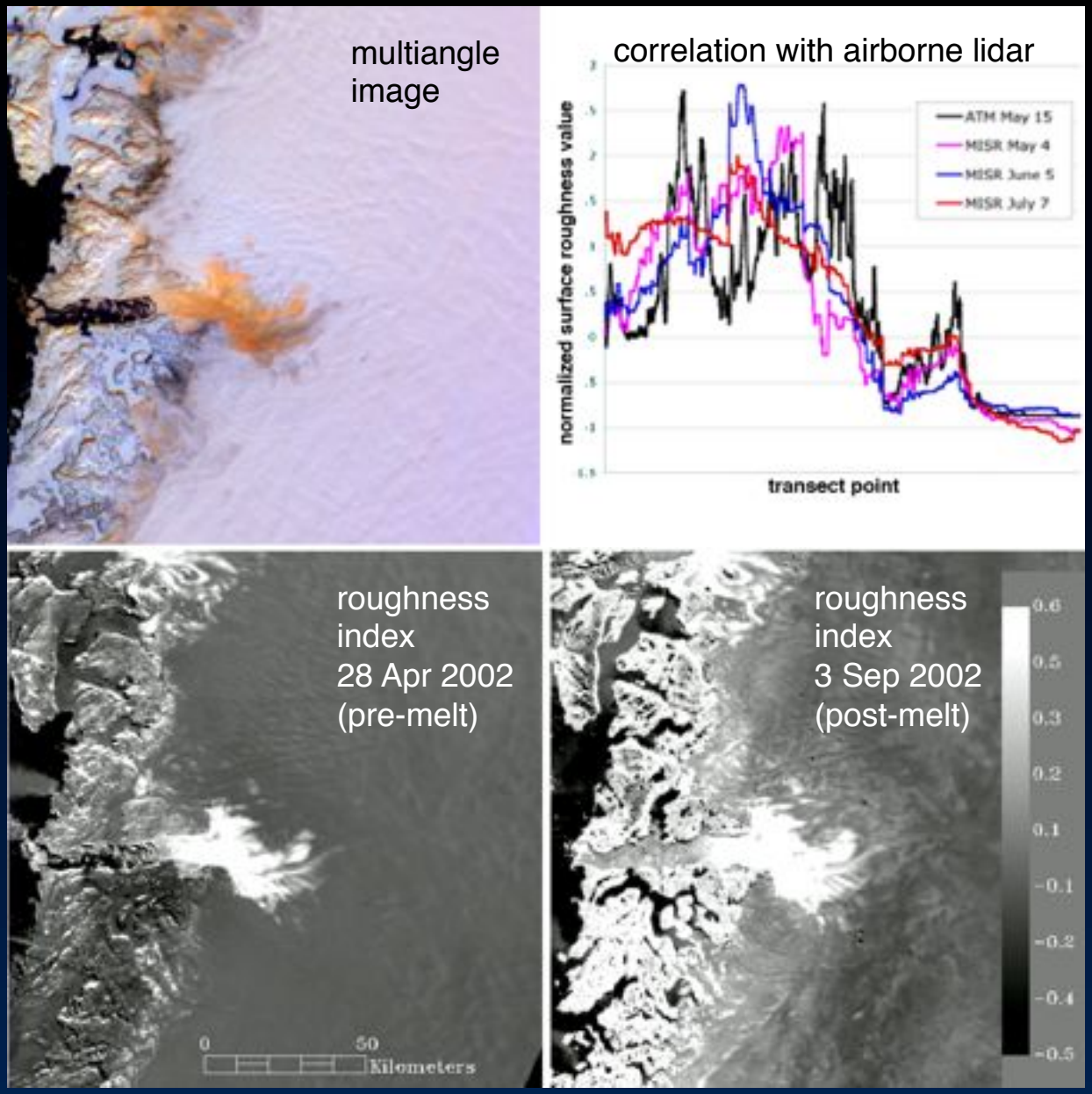

Surface morphology is influenced by ice accumulation, ablation, and melt.

Spatial and temporal changes in ice sheet roughness are revealed in MISR data.

Jakobshavn glacier, Greenland

A. Nolin et al. (2002), TGARS

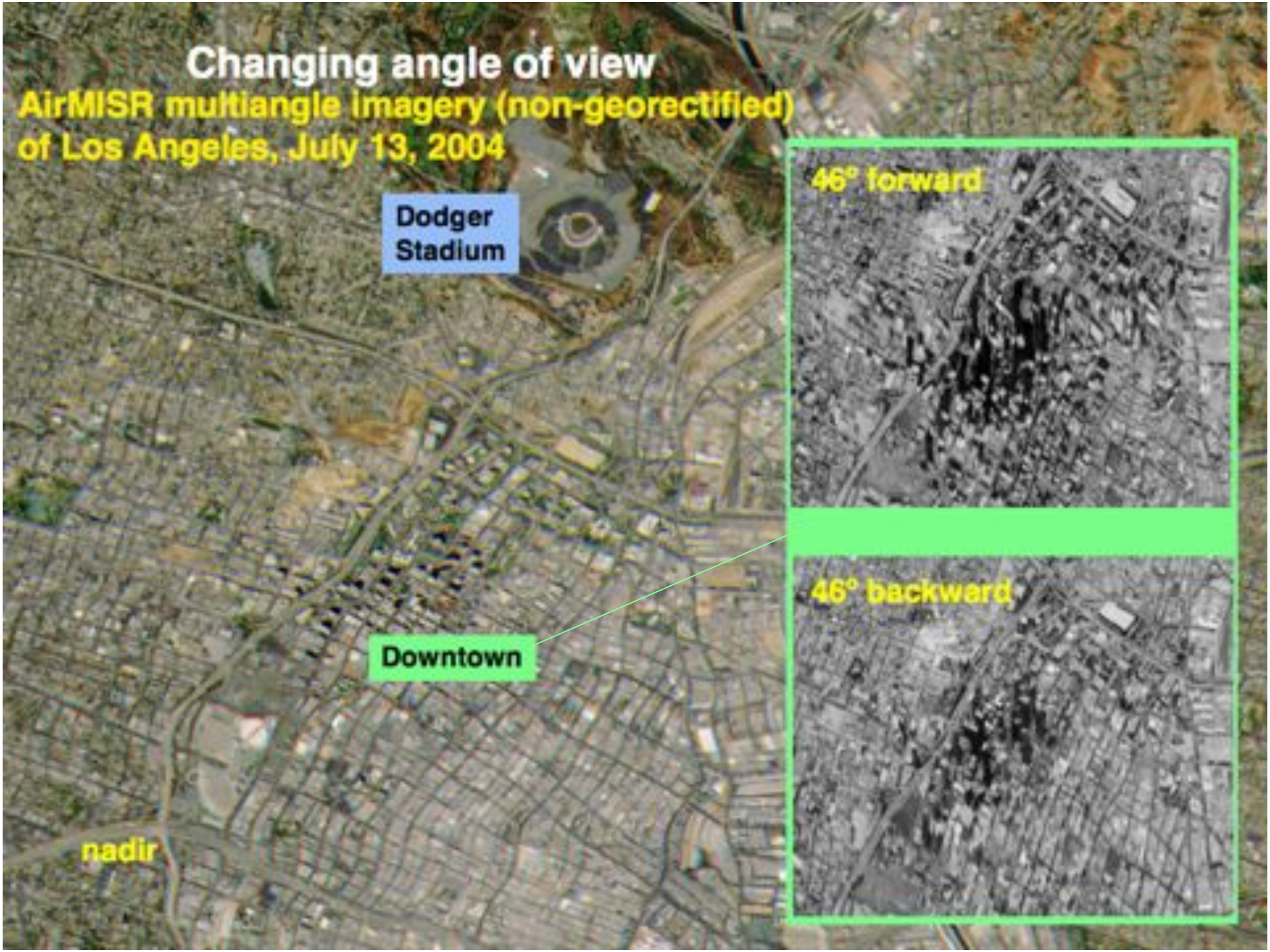
Changing angle of view
AirMISR multiangle imagery (non-georectified)
of Los Angeles, July 13, 2004
Dodger Stadium
46° forward
46° backward
Downtown
nadir

Textural effect is also observable in MISR data

Single spectral band (red)
Display as red: 46° fwd (forward scatter)
Display as green: nadir
Display as blue: 46° aft (backward scatter)

Midtown Manhattan and financial district have reduced forward scatter and more backscatter

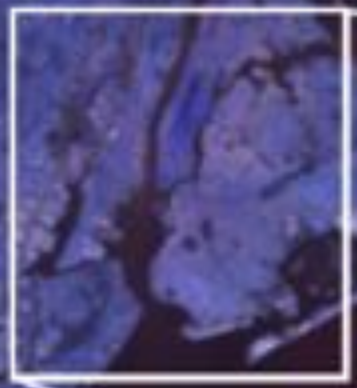

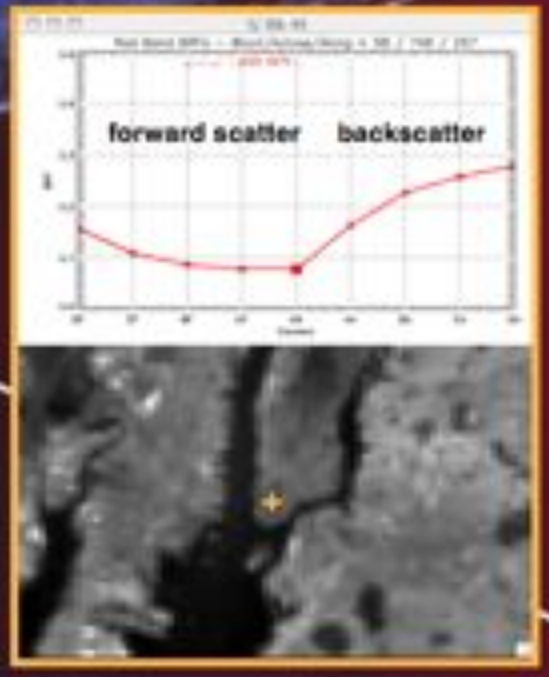

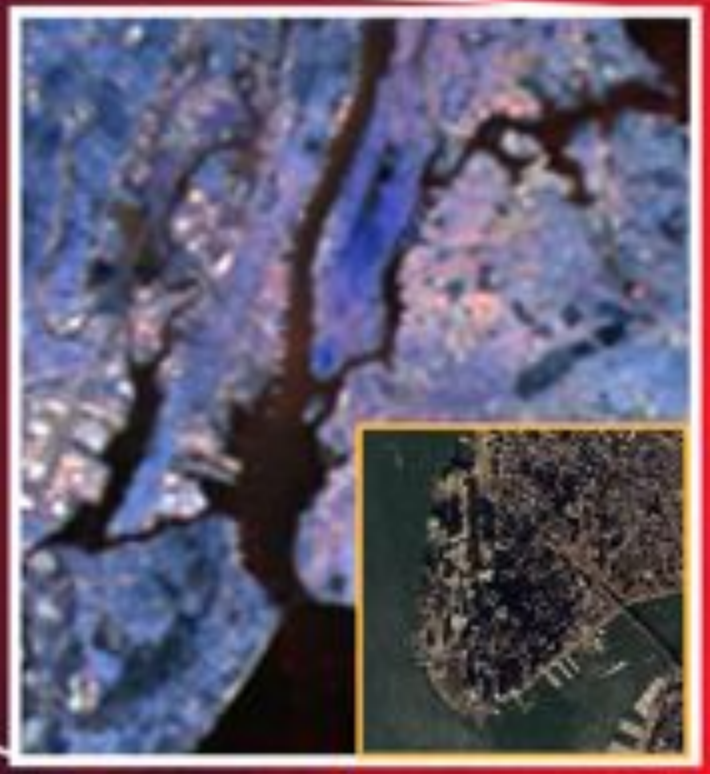

Vegetation canopy heights

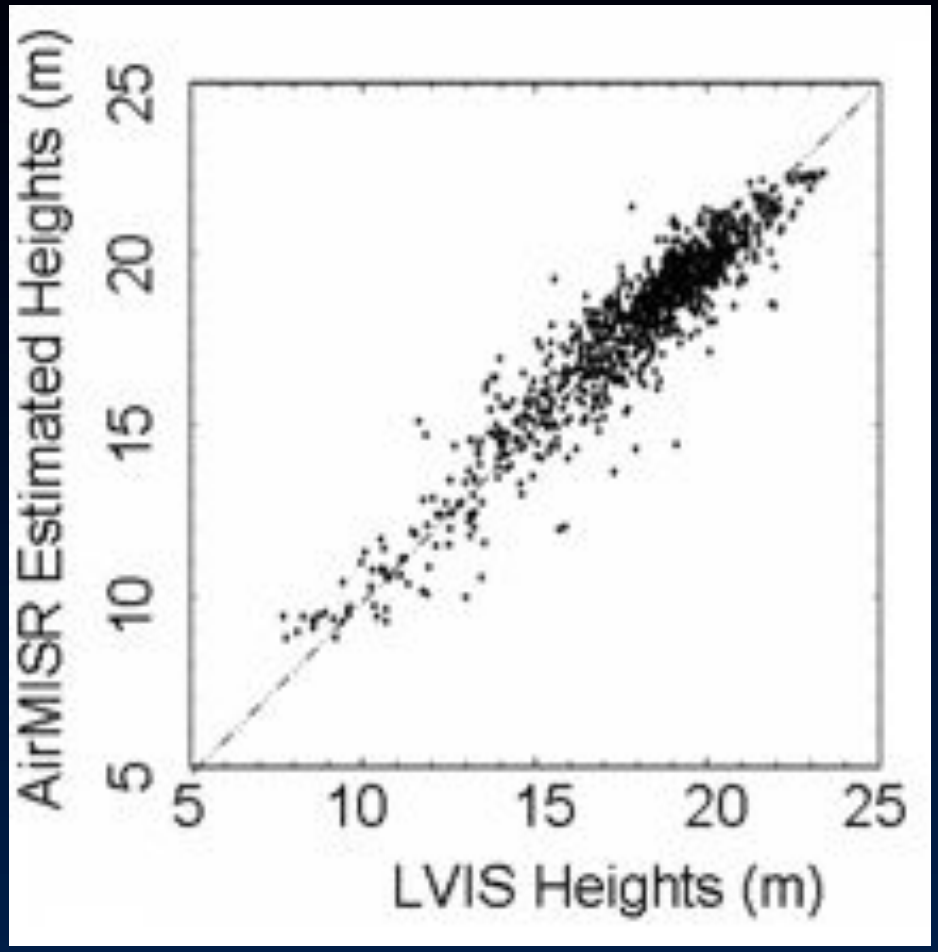

Neural-net derived multiangle height predictor vs. lidar height using airborne (AirMISR/LVIS) data over Maine

Testing with MISR and GLAS is in progress

Kimes et al. (2006), Rem. Sens. Environ.


Cape Hatteras, NC
11 October 2000
26° aft red, green, blue


Cape Hatteras, NC
11 October 2000
26° forward red, green, blue

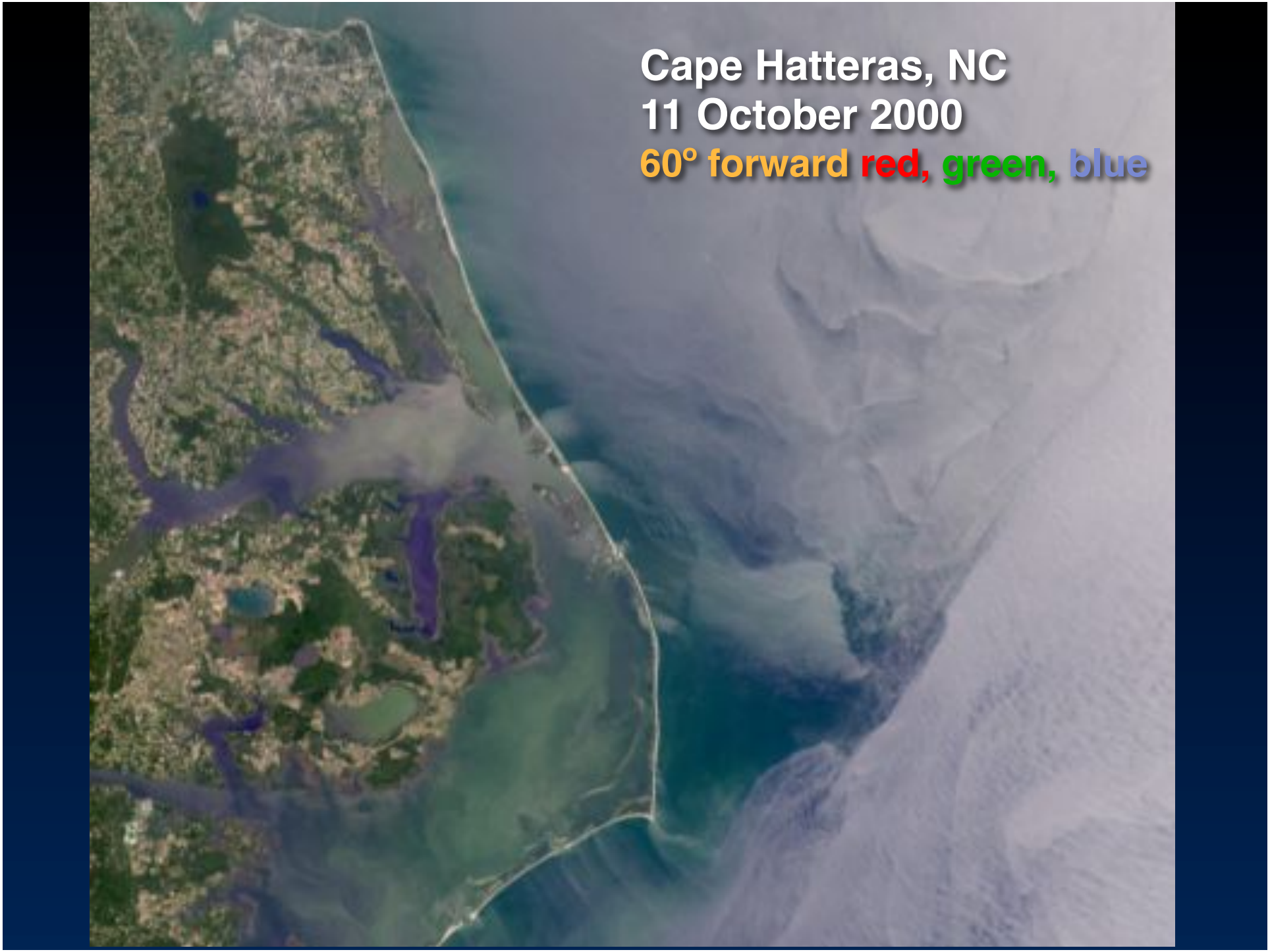
Cape Hatteras, NC
11 October 2000
60° forward red, green, blue

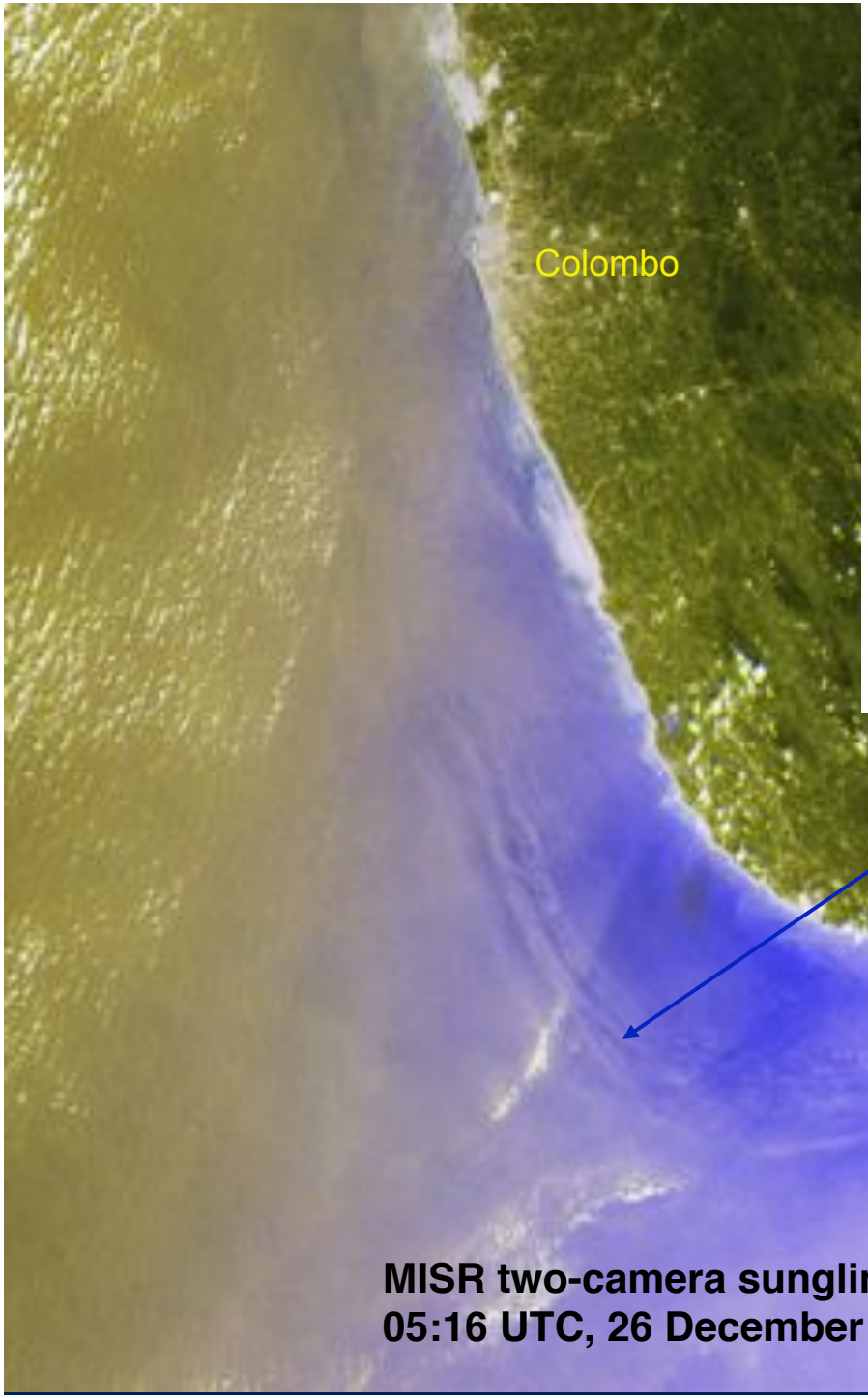

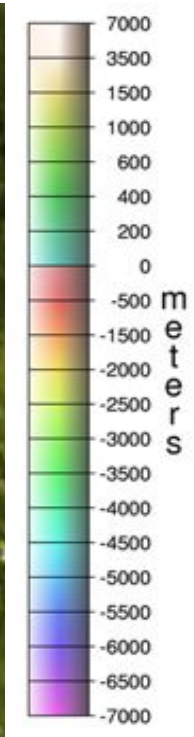

Bathymetry around Sri Lanka
http://topex.ucsd.edu/marine_topo/

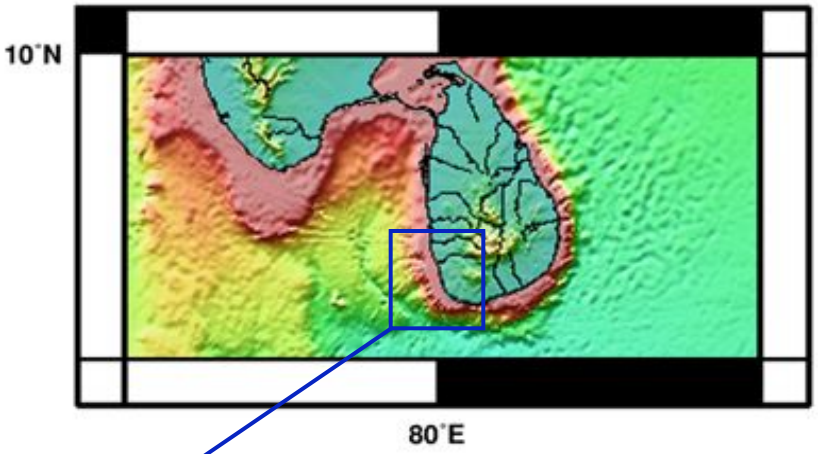

MISR two-camera sunglint composite
05:16 UTC, 26 December 2004

Tsunami-induced waves 30-40 km off SW Sri Lanka coast

Wave pattern is not seen on other dates

Wave location is coincident with dropoff in continental shelf

Waves are slow-moving

Bidirectional reflectance at top-of-atmosphere

San Joaquin Valley
3 January 2001

nadir

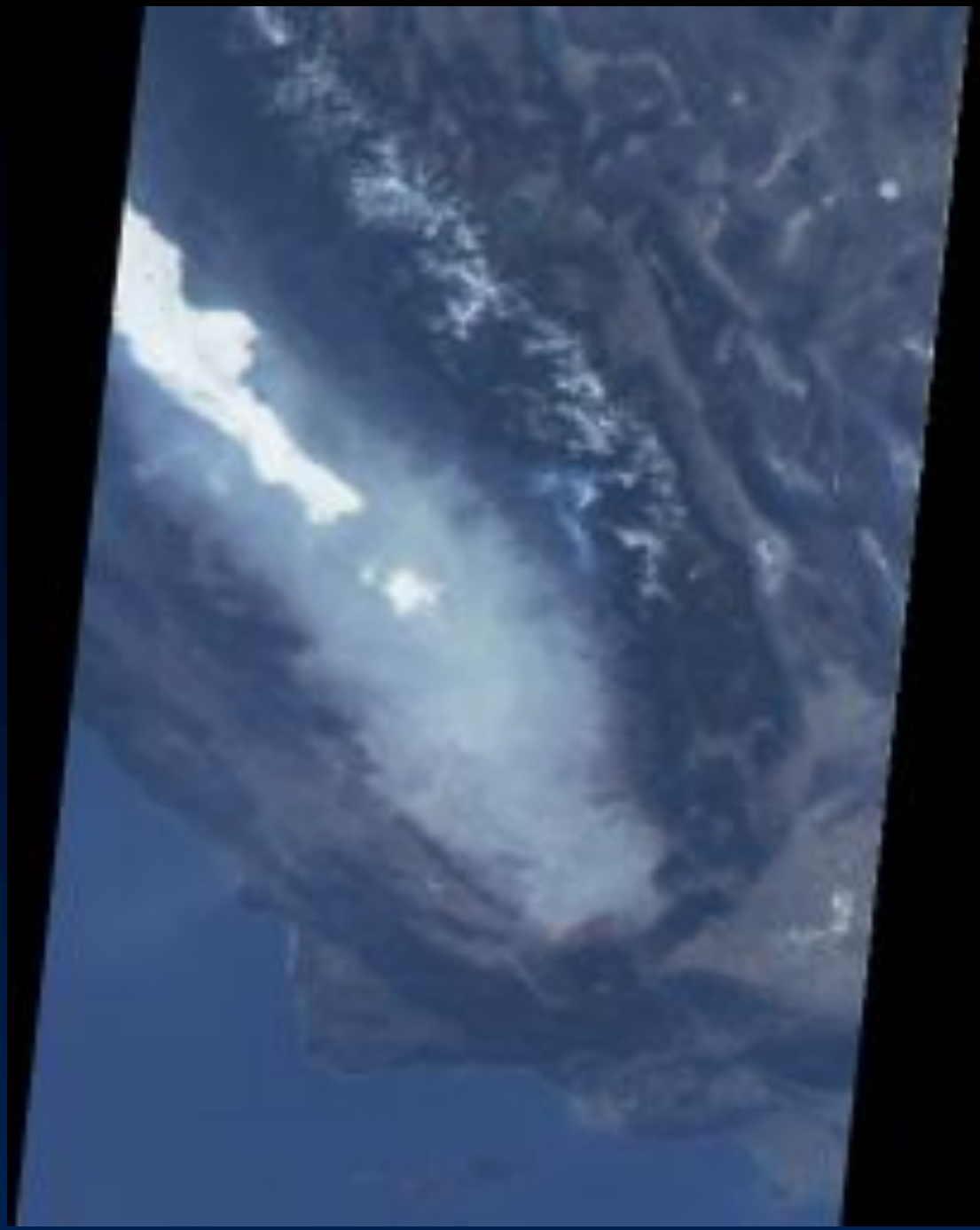

Bidirectional reflectance at top-of-atmosphere

San Joaquin Valley
3 January 2001

70° forward

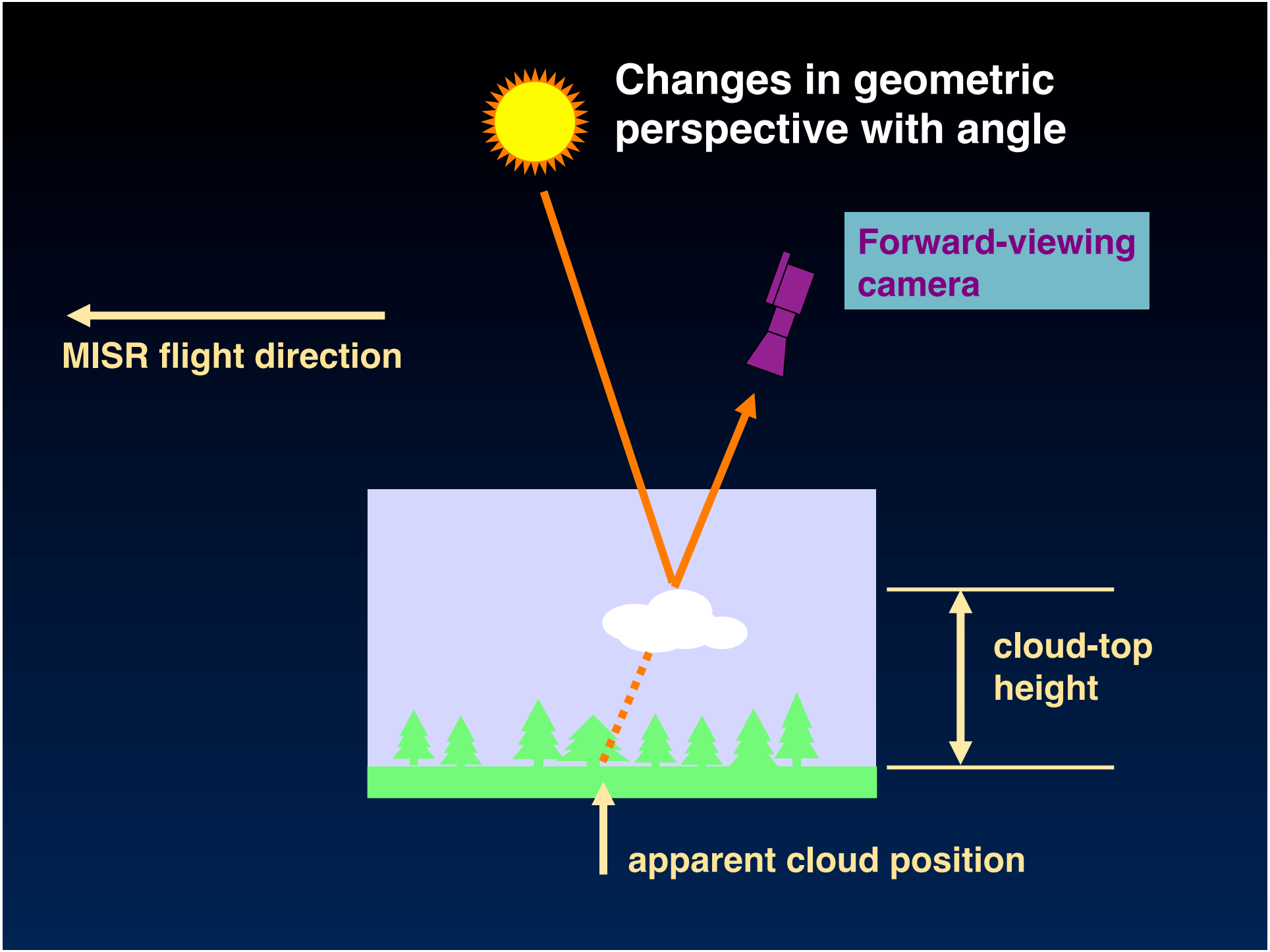
Changes in geometric perspective with angle
Forward-viewing camera
MISR flight direction
cloud-top height
apparent cloud position

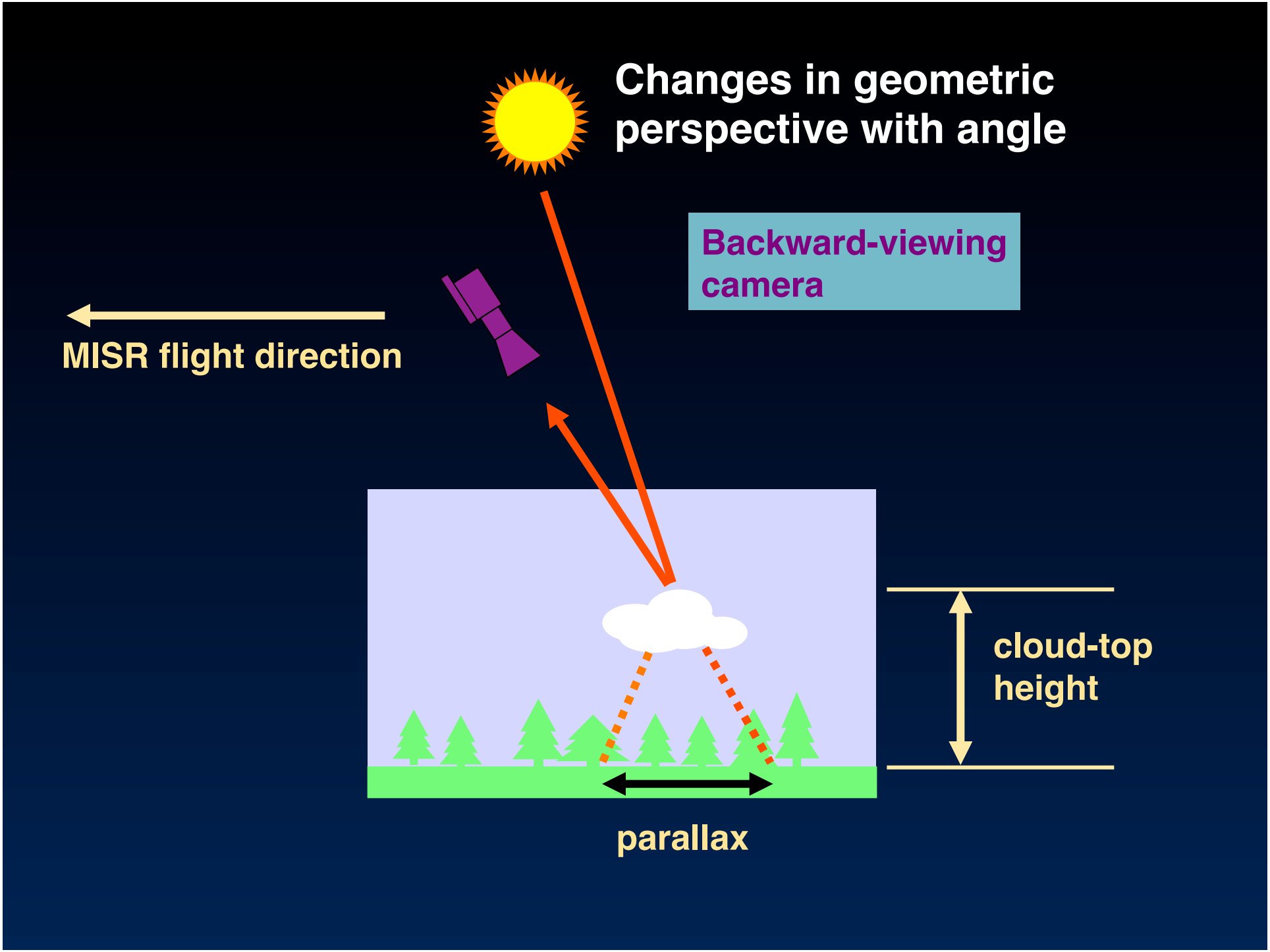
Changes in geometric perspective with angle
Backward-viewing camera
MISR flight direction
cloud-top height
parallax

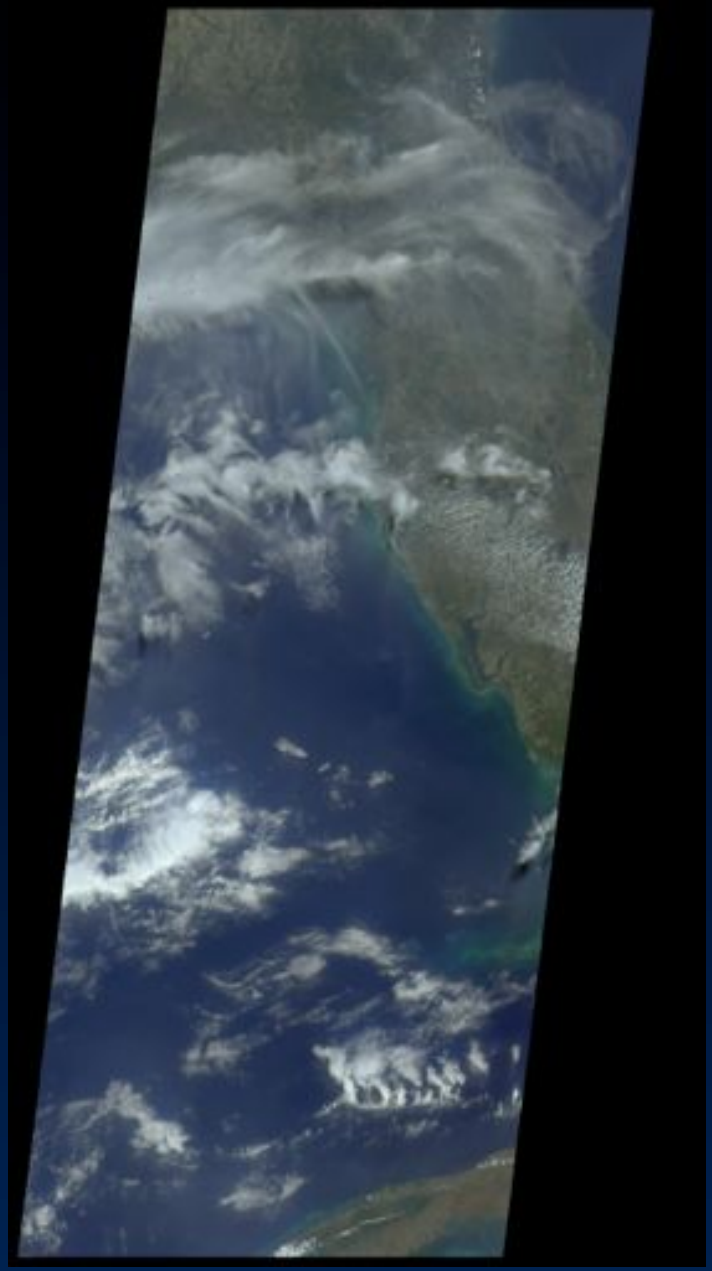

Multiangle “flyover”
Florida and Cuba
6 March 2000

Georgian Bay, Ontario, 6 March 2000

Nadir (An)

70° forward (Df)

Georgian Bay, Ontario, 6 March 2000

Nadir (An)

60° forward (Cf)

Georgian Bay, Ontario, 6 March 2000

Nadir (An)

46° forward (Bf)

Georgian Bay, Ontario, 6 March 2000

Nadir (An)

26° forward (Af)

Cloud reflection in water

Less oblique MISR camera

MISR flight direction

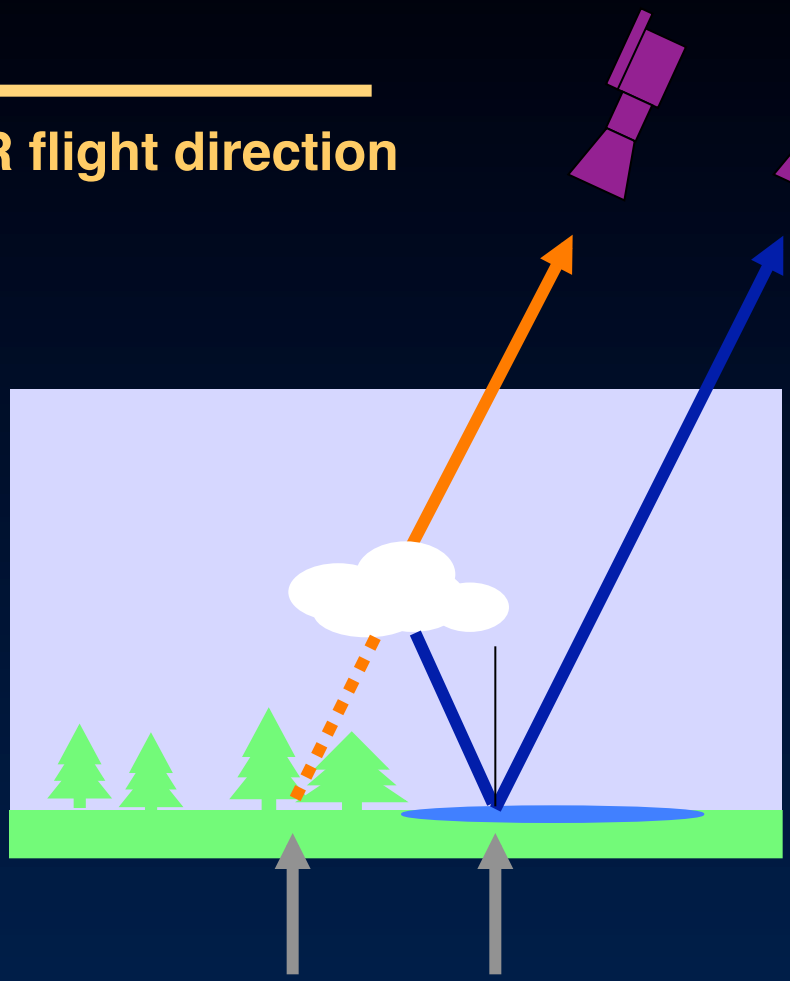

apparent cloud position

reflection position

Cloud reflection in water

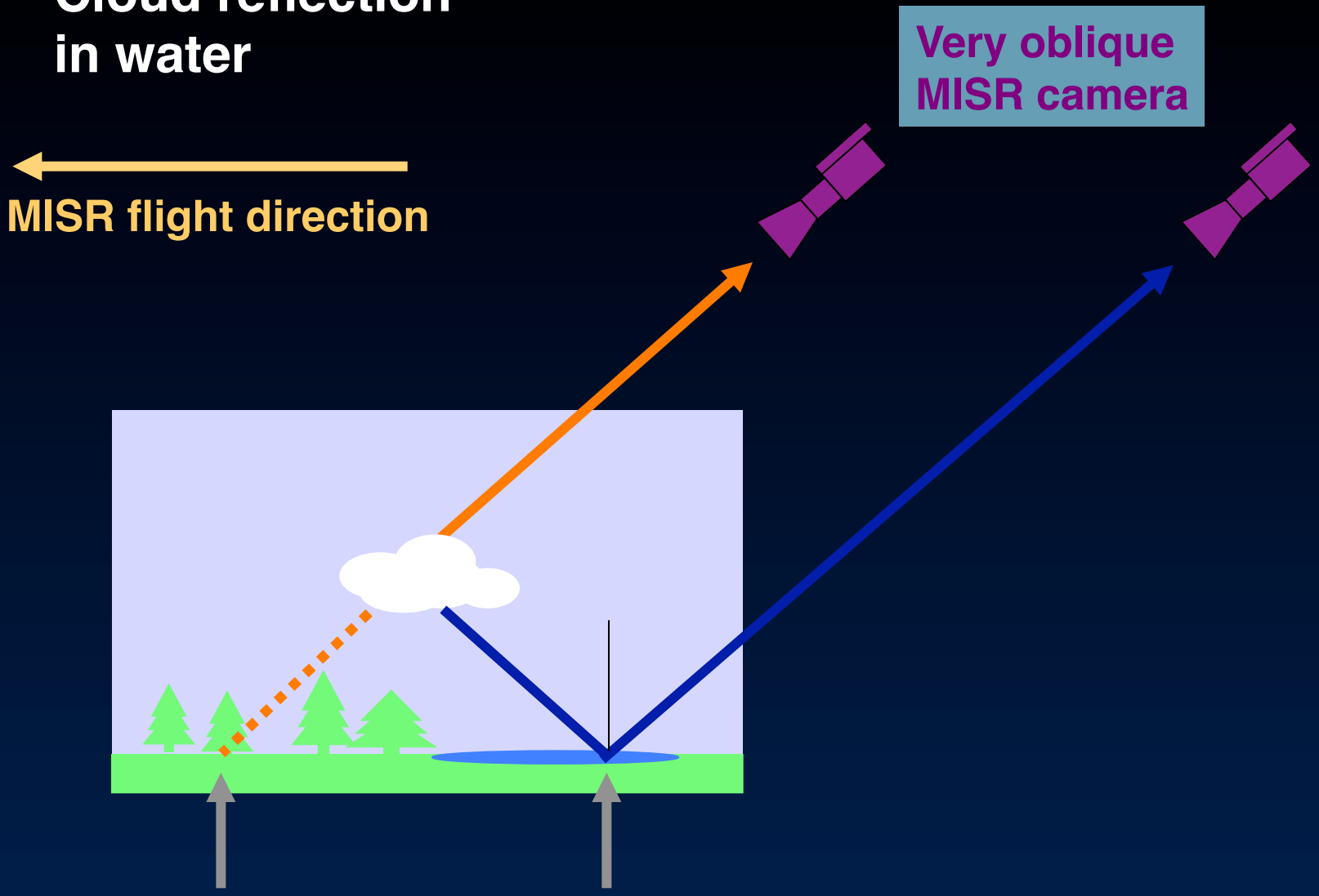

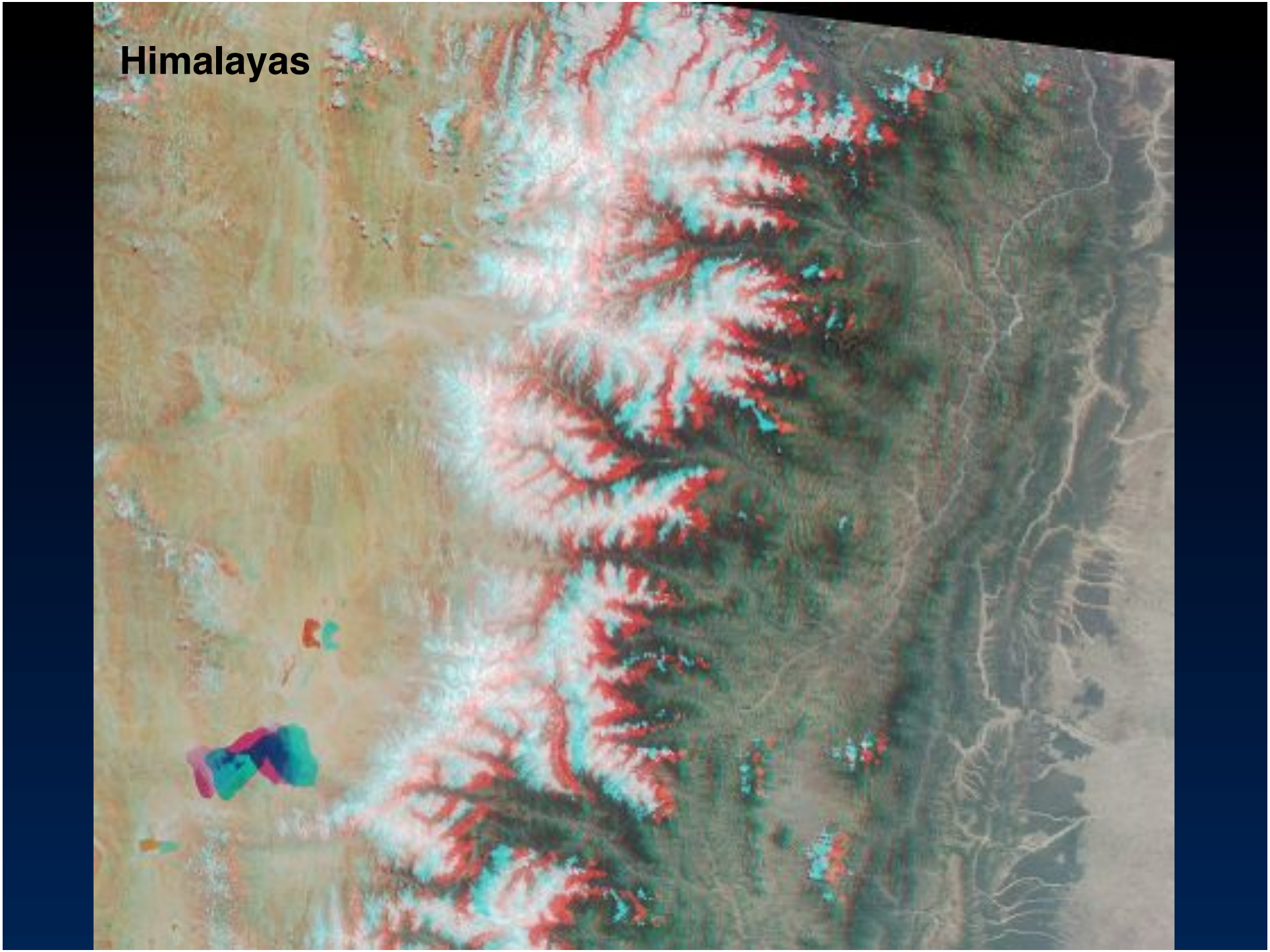
Himalayas

Eruption of Mt. Etna, 22 July 2001

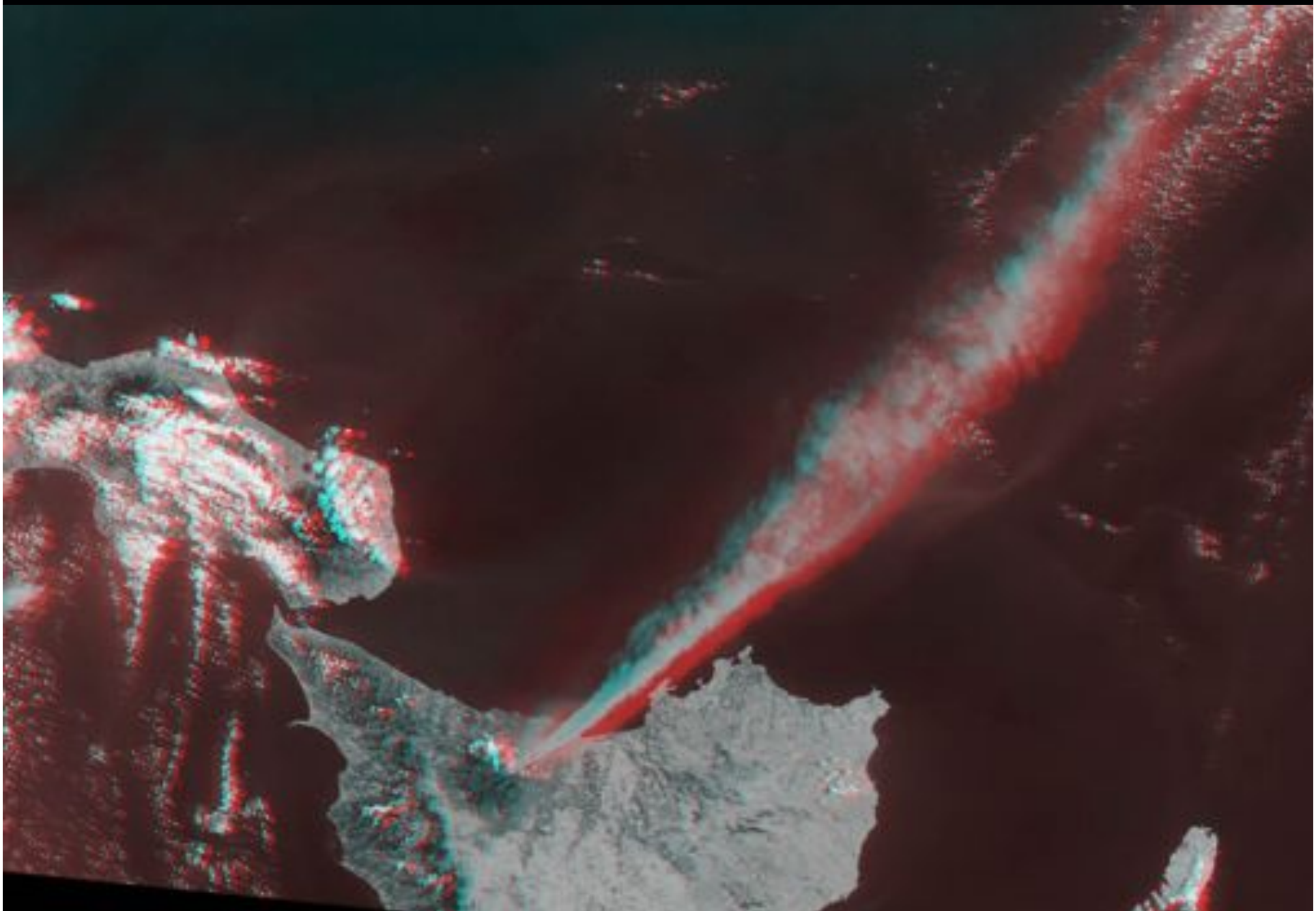

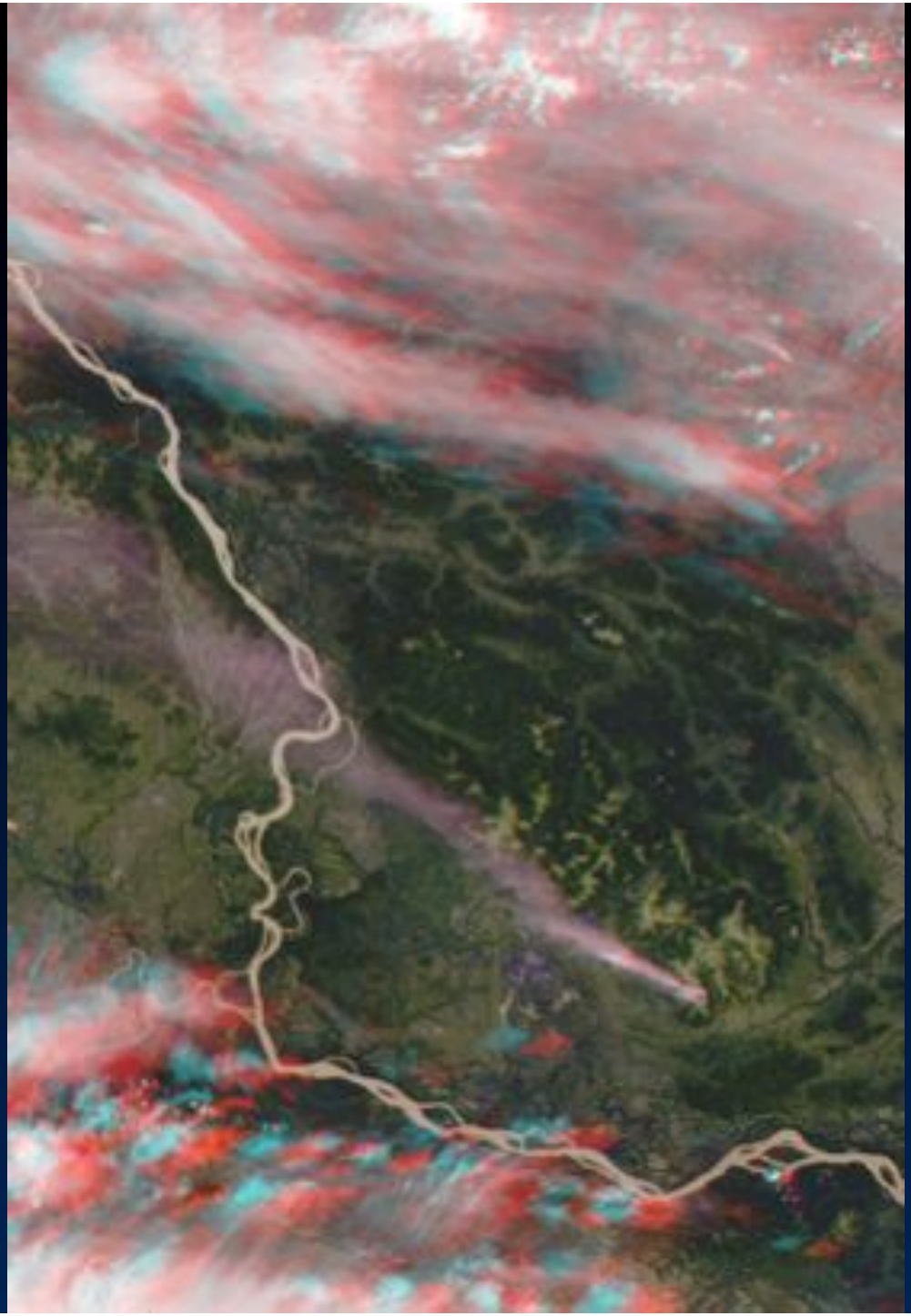

Alaskan Wildfire and Cirrus Clouds

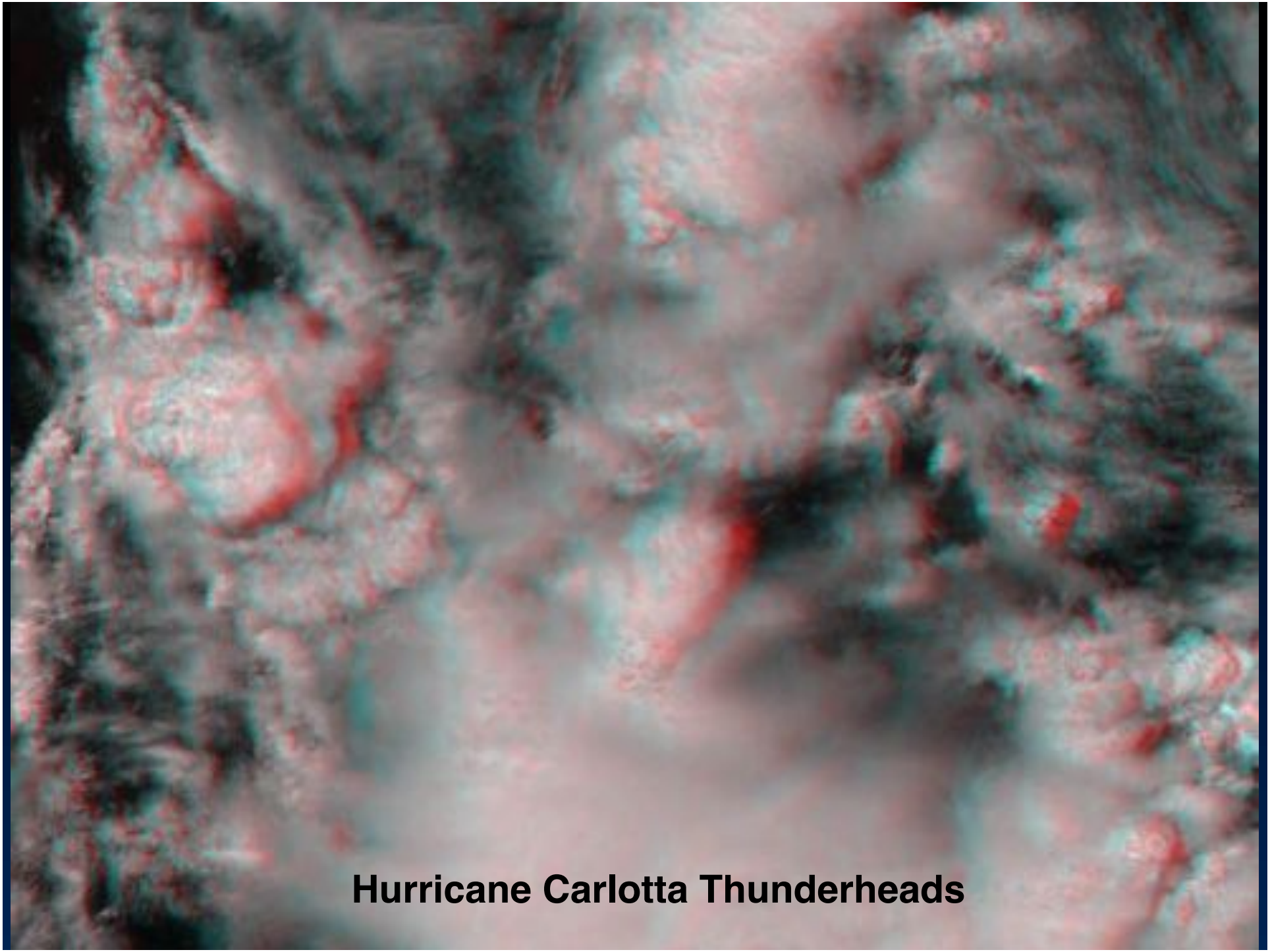

Hurricane Carlotta Thunderheads

Hurricane Alberto Eye

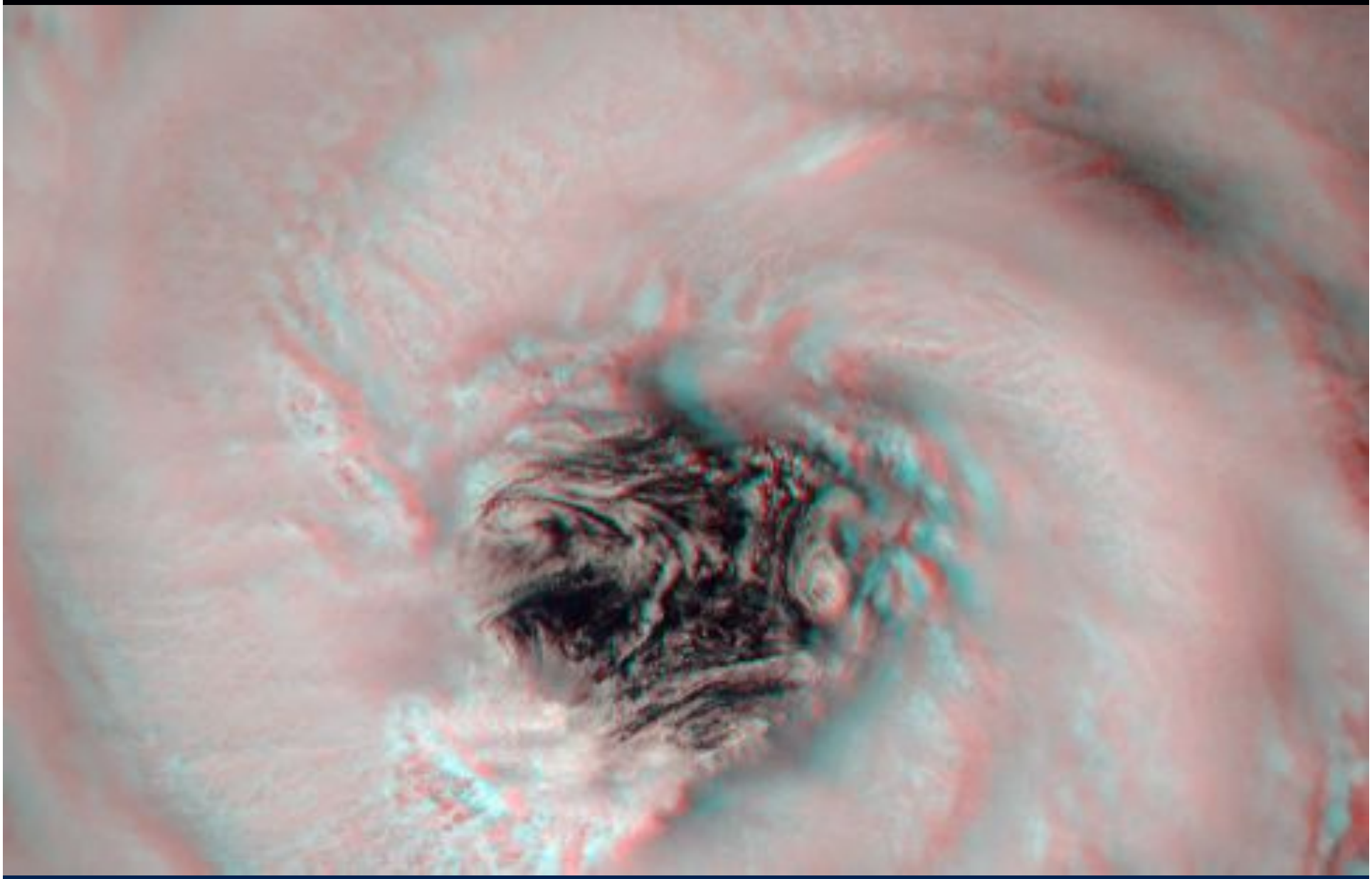

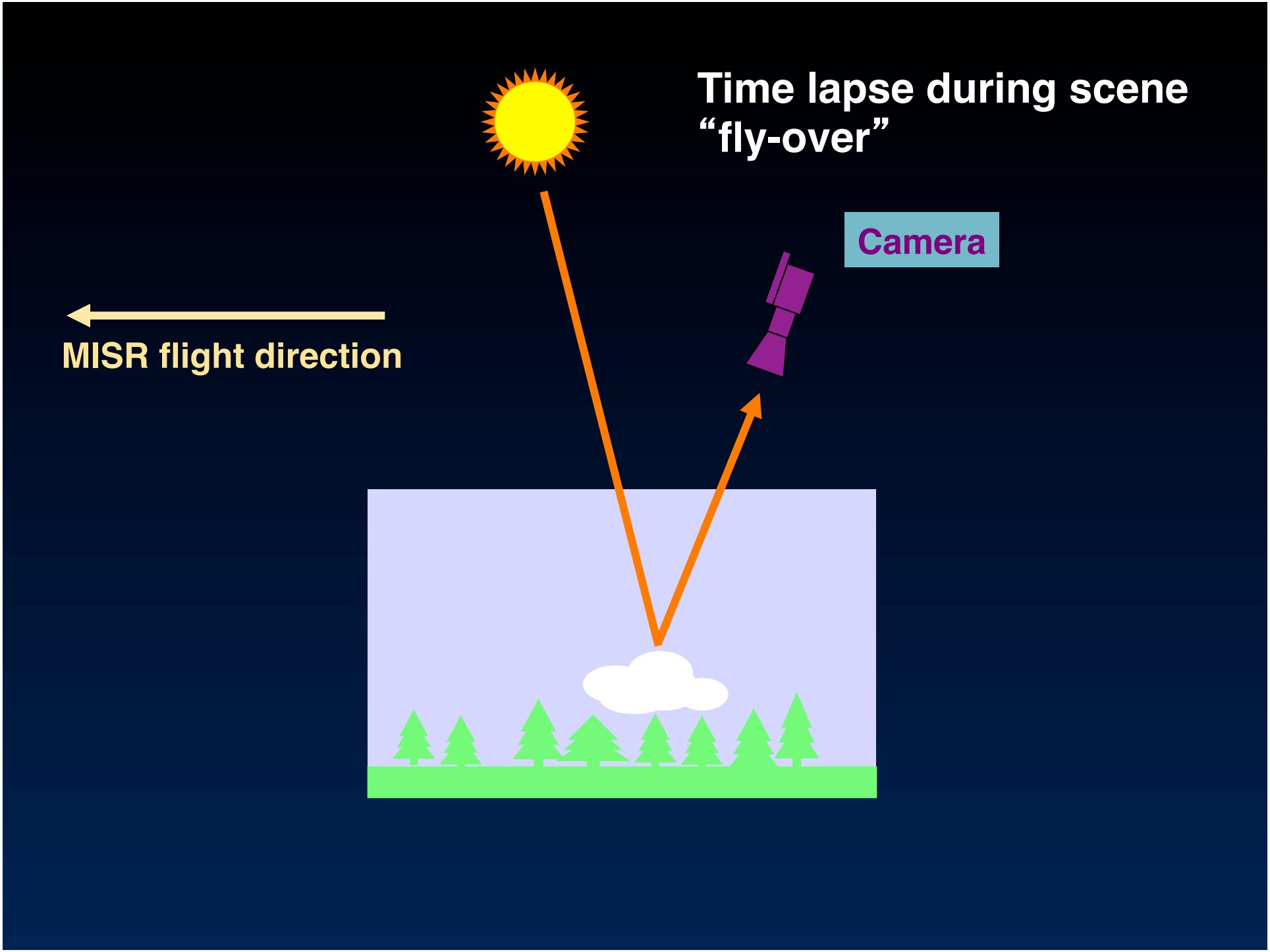
Time lapse during scene
“fly-over”
Camera
MISR flight direction

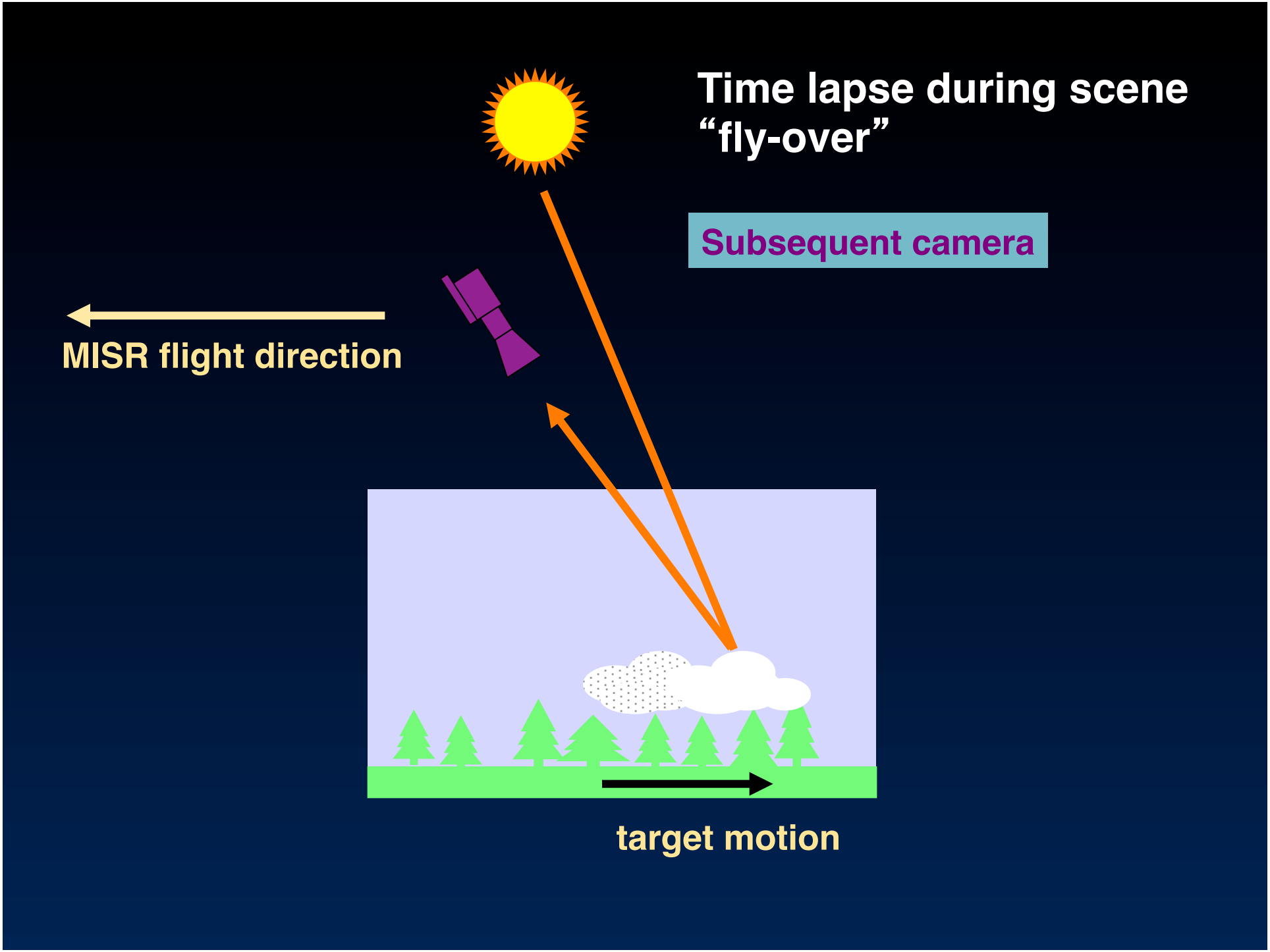
Time lapse during scene
“fly-over”
Subsequent camera
MISR flight direction
target motion

Moving ships off the North Carolina Coast

11 October 2000

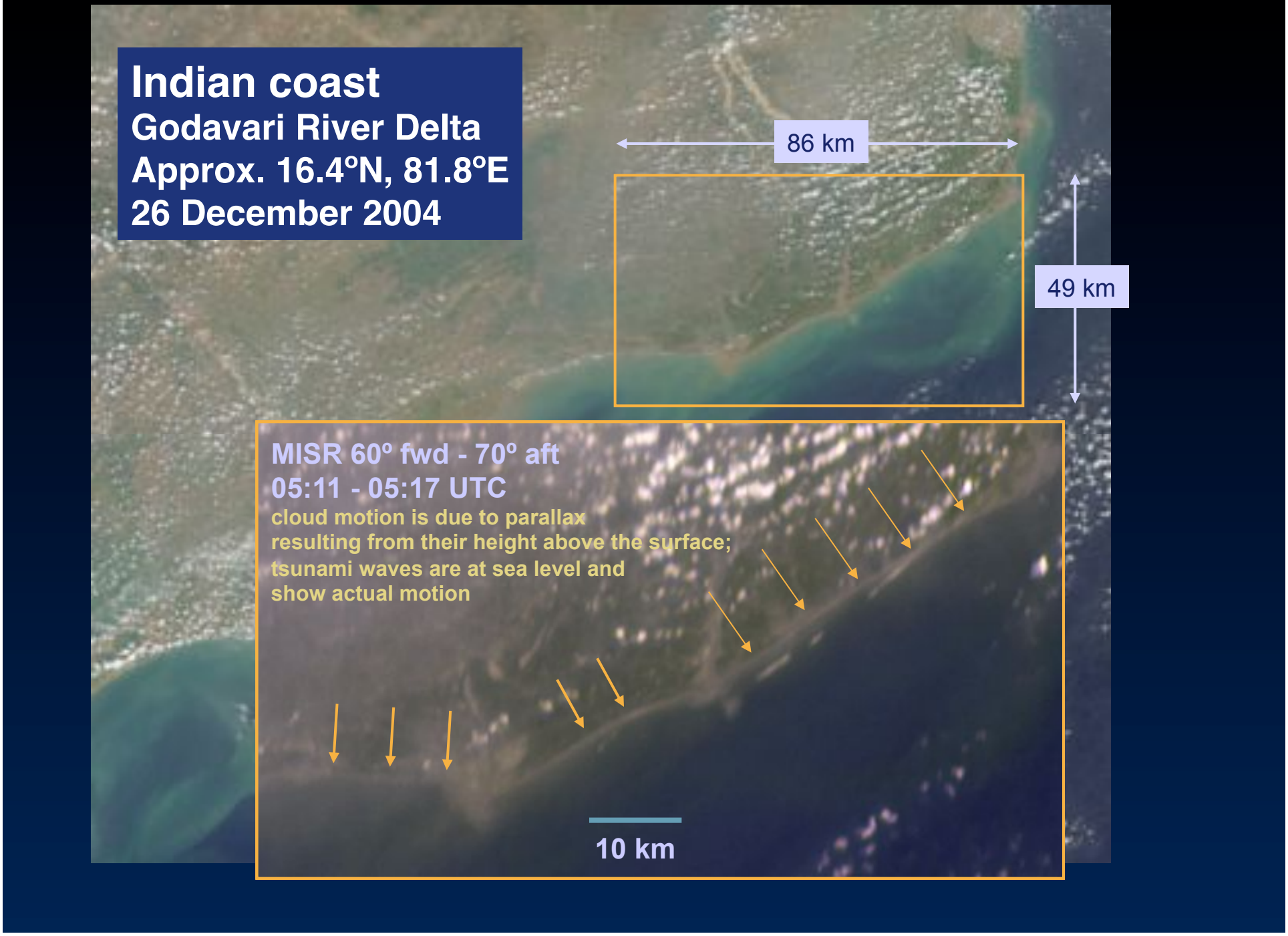
Indian coast
Godavari River Delta
Approx. 16.4°N, 81.8°E
26 December 2004
86 km
49 km
MISR 60° fwd - 70° aft
05:11 - 05:17 UTC
cloud motion is due to parallax
resulting from their height above the surface;
tsunami waves are at sea level and
show actual motion
10 km

L1B2 Geometric Parameters (MIS03)

Provided on 17.6-km centers

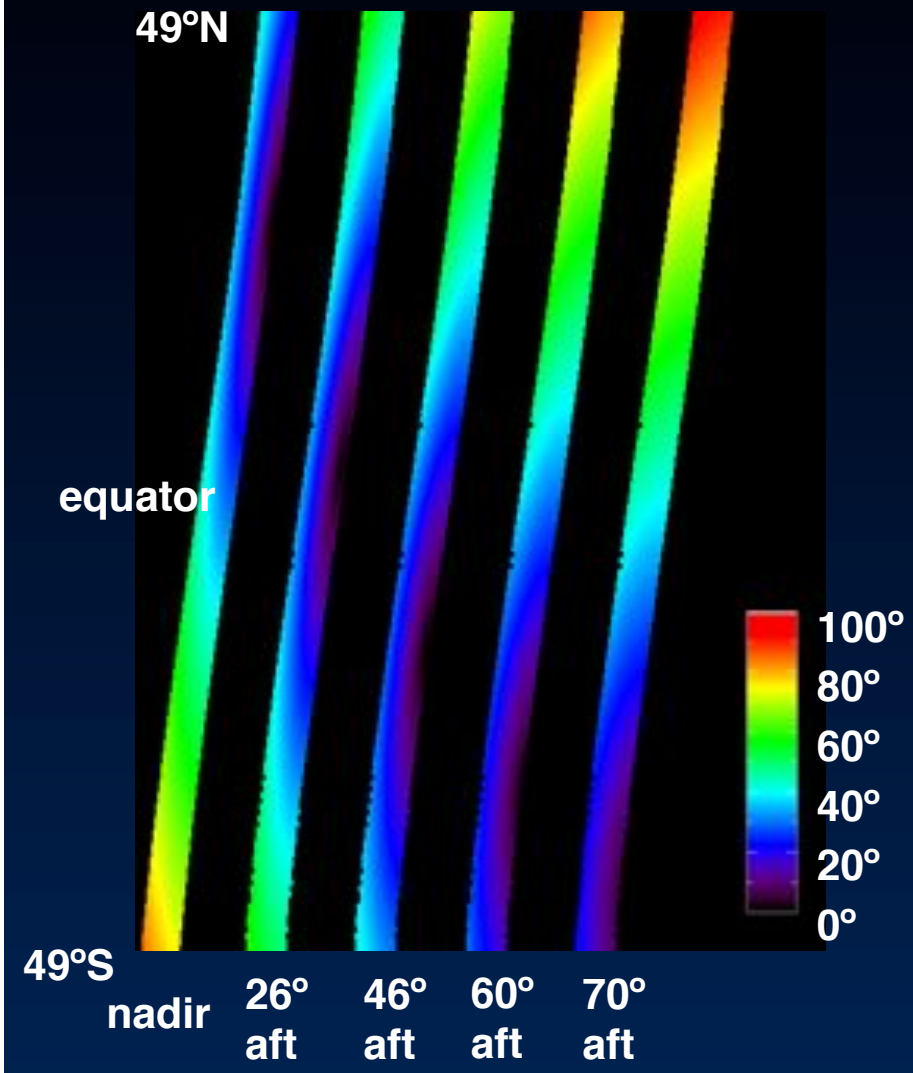

Example of glitter angle July 3

CONTENTS

- View zenith and azimuth angles per camera; azimuths measured relative to local north
- Solar zenith and azimuth angles correspond to midpoint viewing time of only those cameras which observed the point
- Scatter and glitter angles also included in product

Level 2 Standard Products

Level 2 standard products

- Level 2TC stereo
- Level 2TC cloud classifiers
- Level 2TC top-of-atmosphere albedo
- Level 2AS aerosol
- Level 2AS land surface

Level 2 processing uses multiple cameras simultaneously

- Angular radiance signatures
- Geometric parallax
- Time lapse

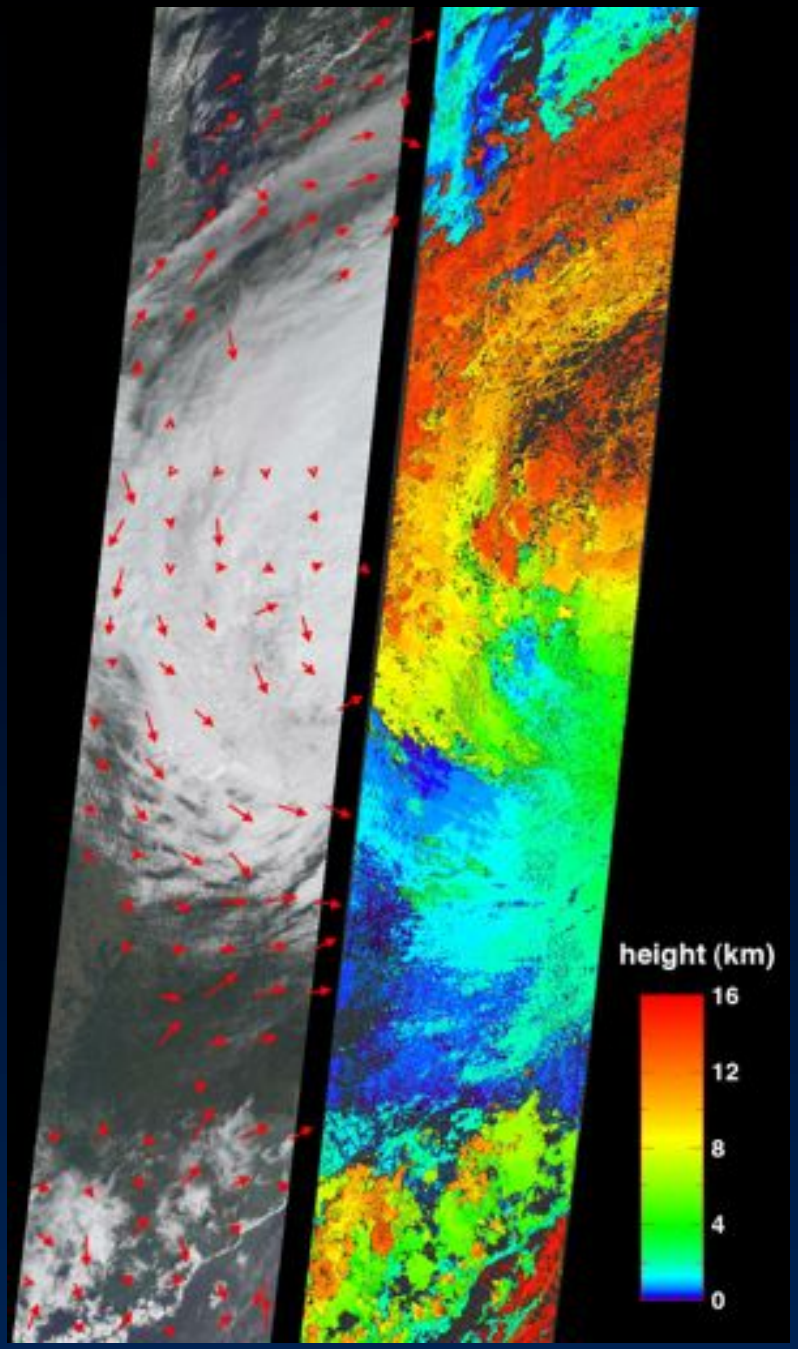

L2 TOA/Cloud Stereo Product (MIS04)

Cloud heights and cloud-tracked winds

HEIGHT ATTRIBUTES

- 1.1-km resolution
- Purely geometric retrievals of height
- Independent of temperature profiles and cloud emissivity
- Independent of radiometric calibration
- Accuracy 500 -1000 m

WIND ATTRIBUTES

- 70.4-km resolution
- Uses stereo triplets
- Accuracy 1-3 m/s with 300 m height resolution

Hurricane Katrina
30 August 2005

Tropical Cyclone Monty in Western Australia
29 February and 2 March 2004

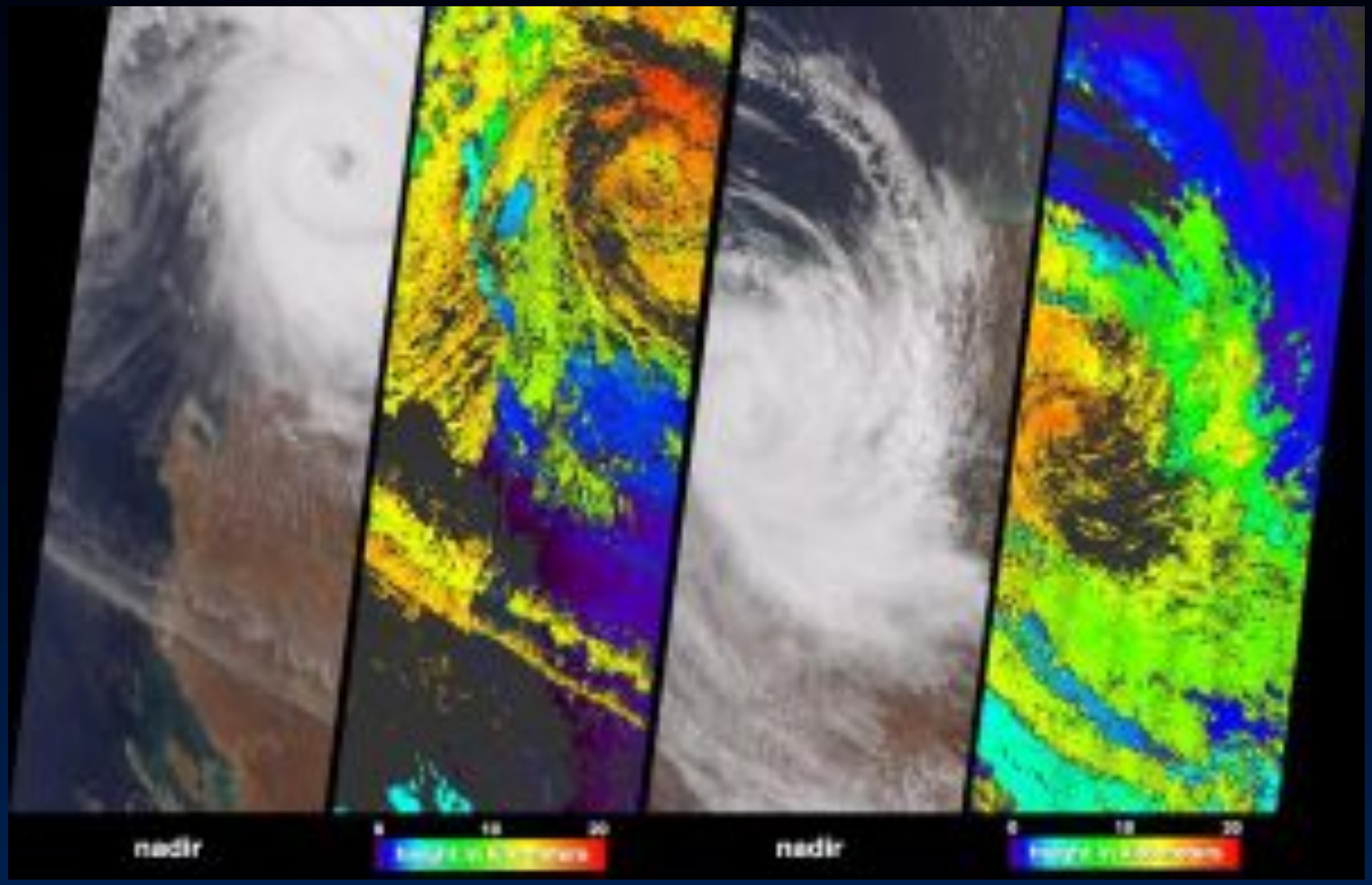

Measuring wildfire smoke plume injection and transport heights

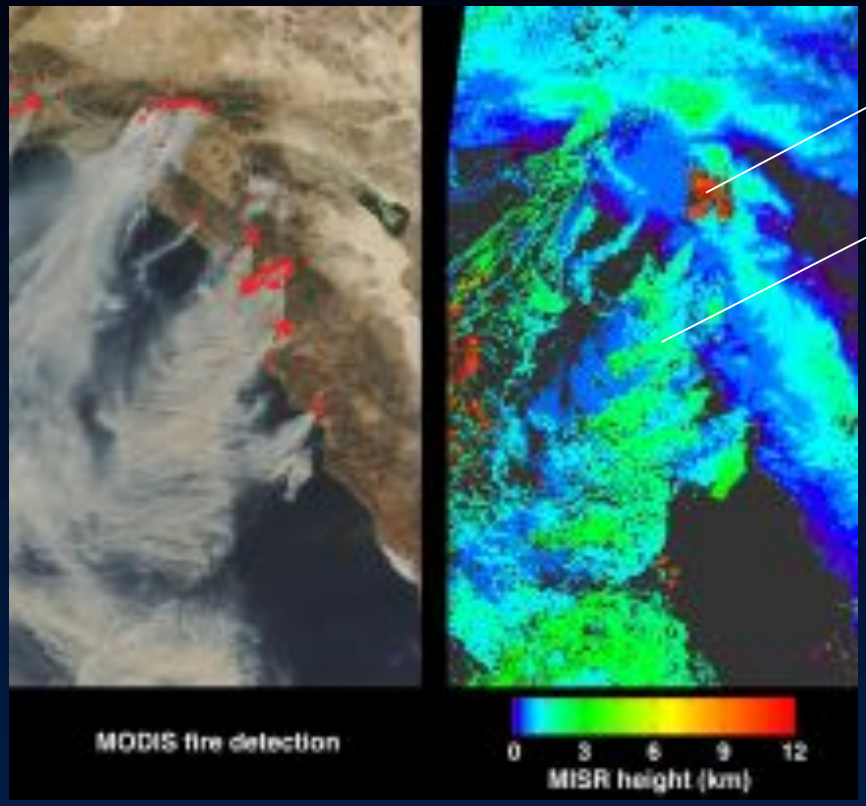

MODIS/MISR data from Terra
26 October 2003

cirrus

smoke

GLAS vertical profiles
28 October 2003

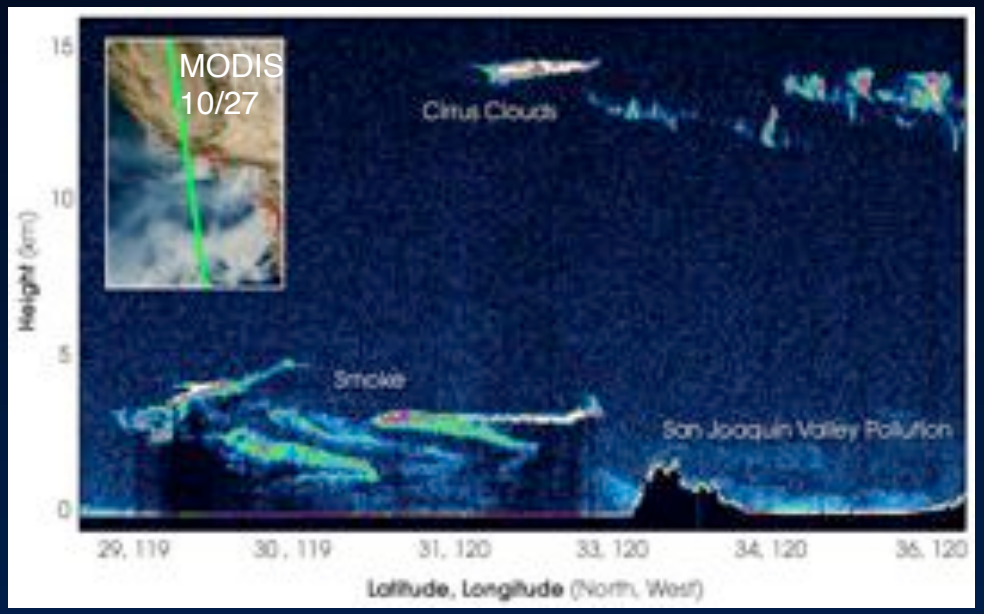

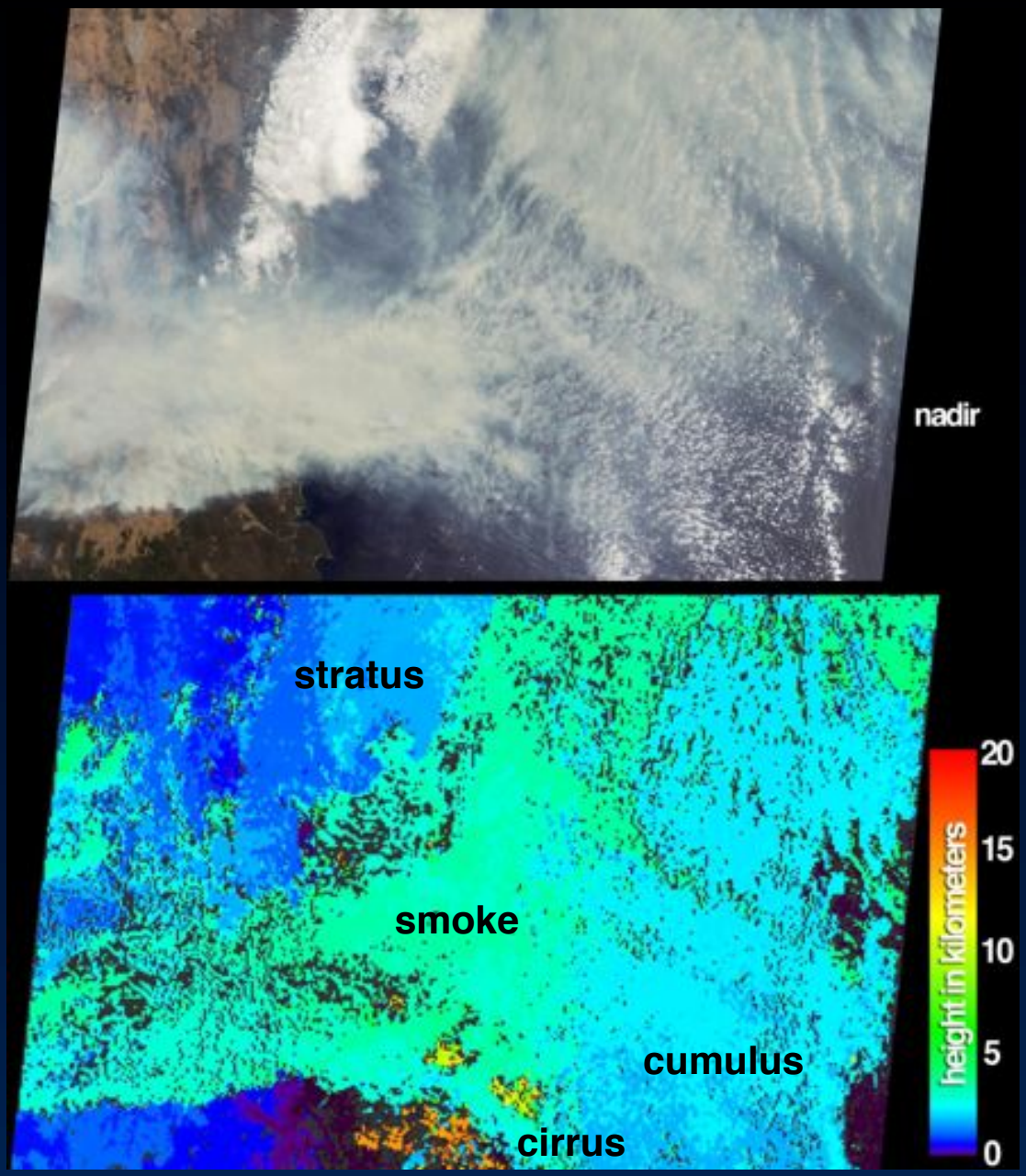

Fires in the Australian Capital Territory

18 January 2003

L2 TOA/Cloud Albedo Product (MIS04)

Cloud-top-projected TOA albedo and bidirectional reflectance

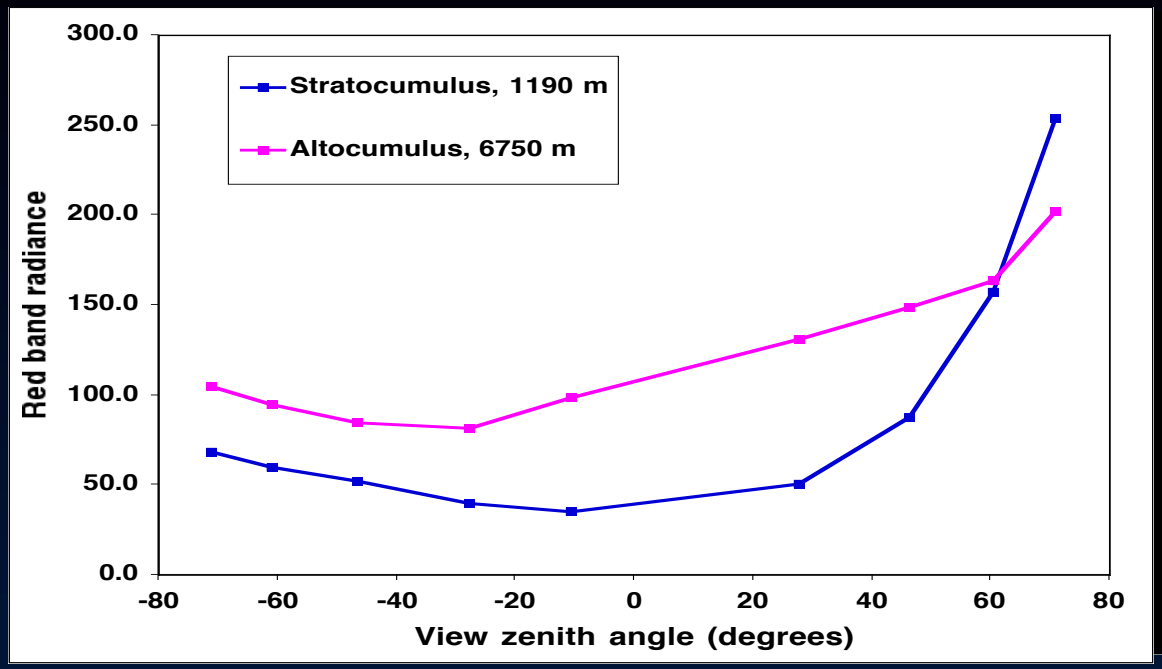

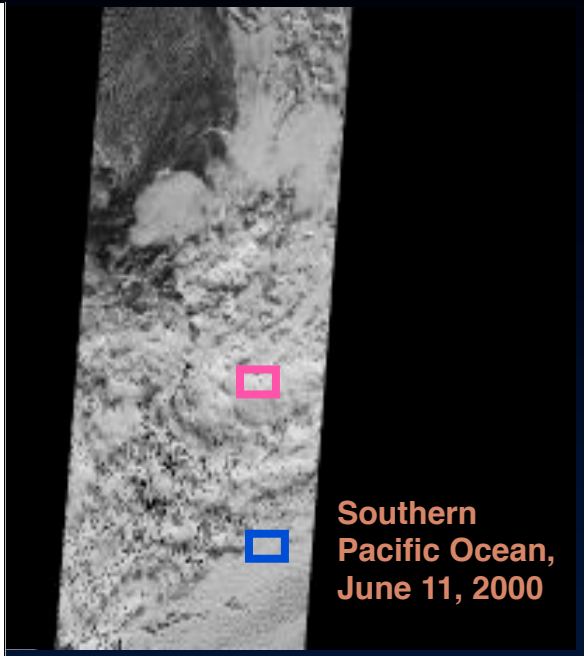

CONTENTS

- "Feature-referenced" top-of-atmosphere bidirectional reflectances
- Includes TOA albedos at fine (2.2. km) resolution for scene classification, and coarse (35.2 km resolution) for mesoscale radiation budget

Multiangle tests of cloud homogeneity

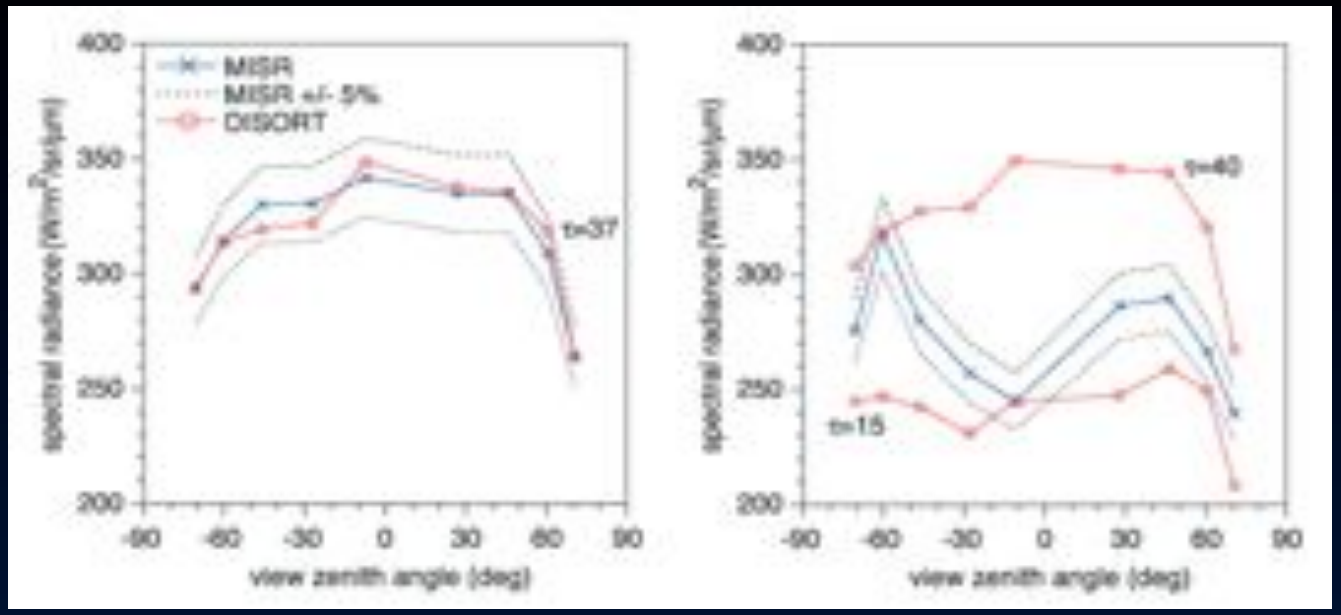

1-D theory fits MISR observations

1-D theory does not fit MISR observations

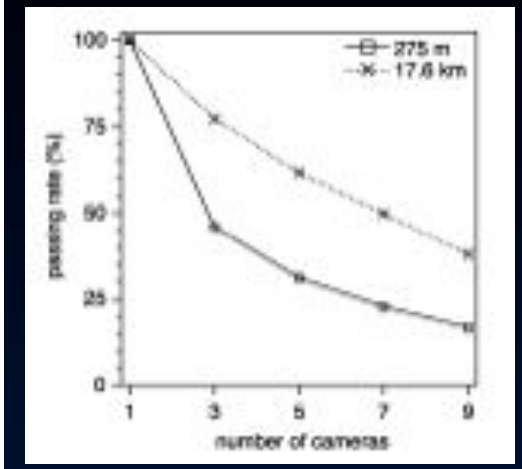

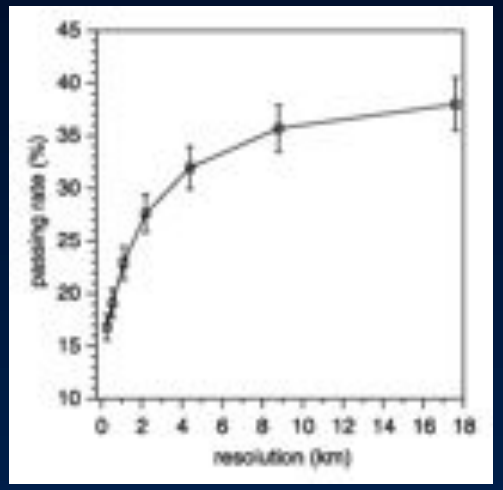

Multiangle data provides a physical consistency check on MODIS 1-D cloud retrieval assumption

Cloud morphology, not just cloud microphysics, plays a major role in determining TOA bidirectional reflectance

A. Horvath, R. Davies (2004), GRL

L2 Aerosol/Surface Product (MIS05)

Aerosol parameters

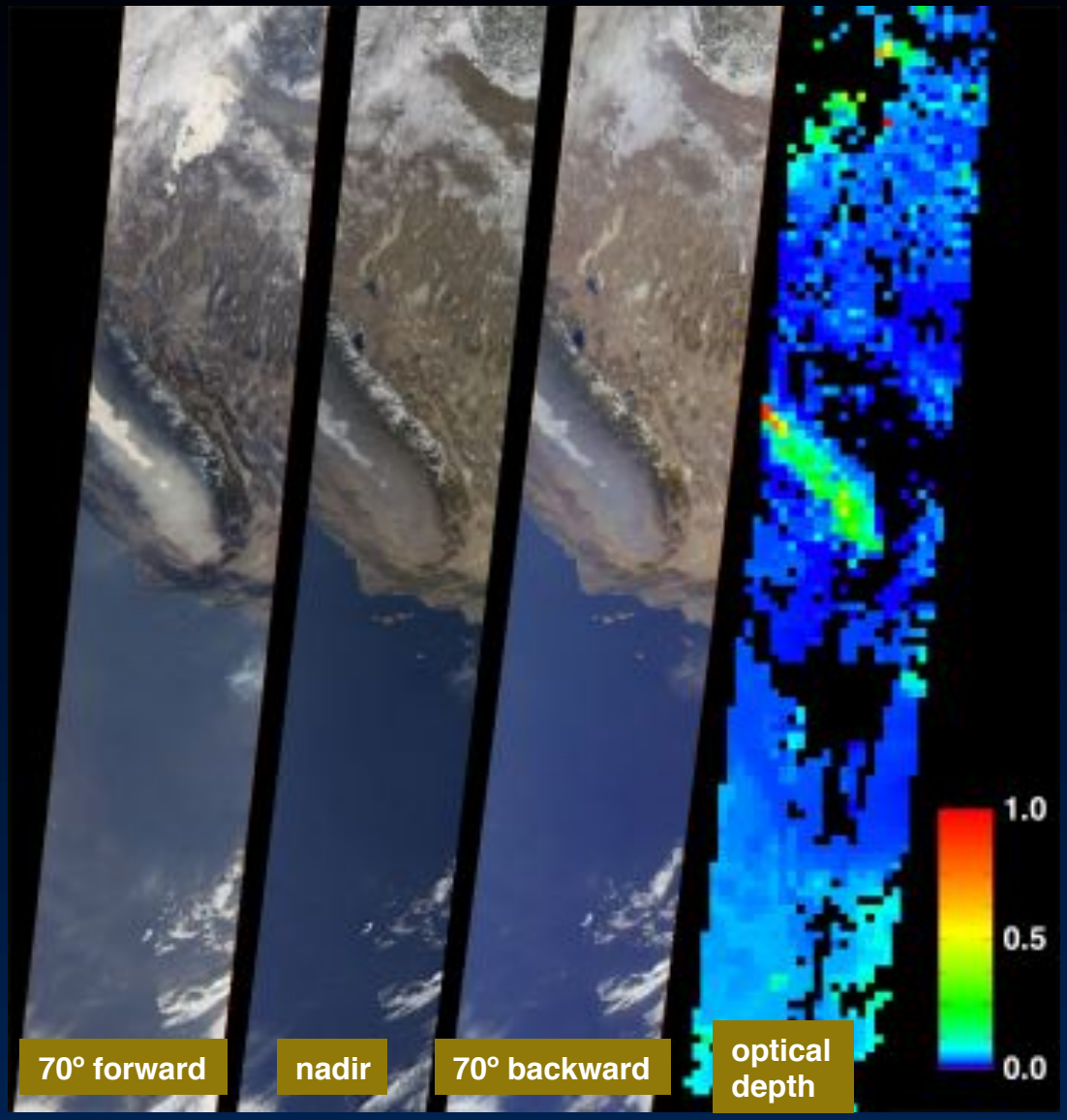

J. Martonchik et al. (2002), TGARS

ATTRIBUTES

- Validation and quality assessment of aerosol optical depth performed
- Validation of aerosol particle properties in progress

  --Angstrom exponent
  --Size binned fractions
  --Single-scattering albedo
  --Sphericity

Southern California and Southwestern Nevada
January 3, 2001

Retrieval of aerosol optical depth over a wide range of surface types

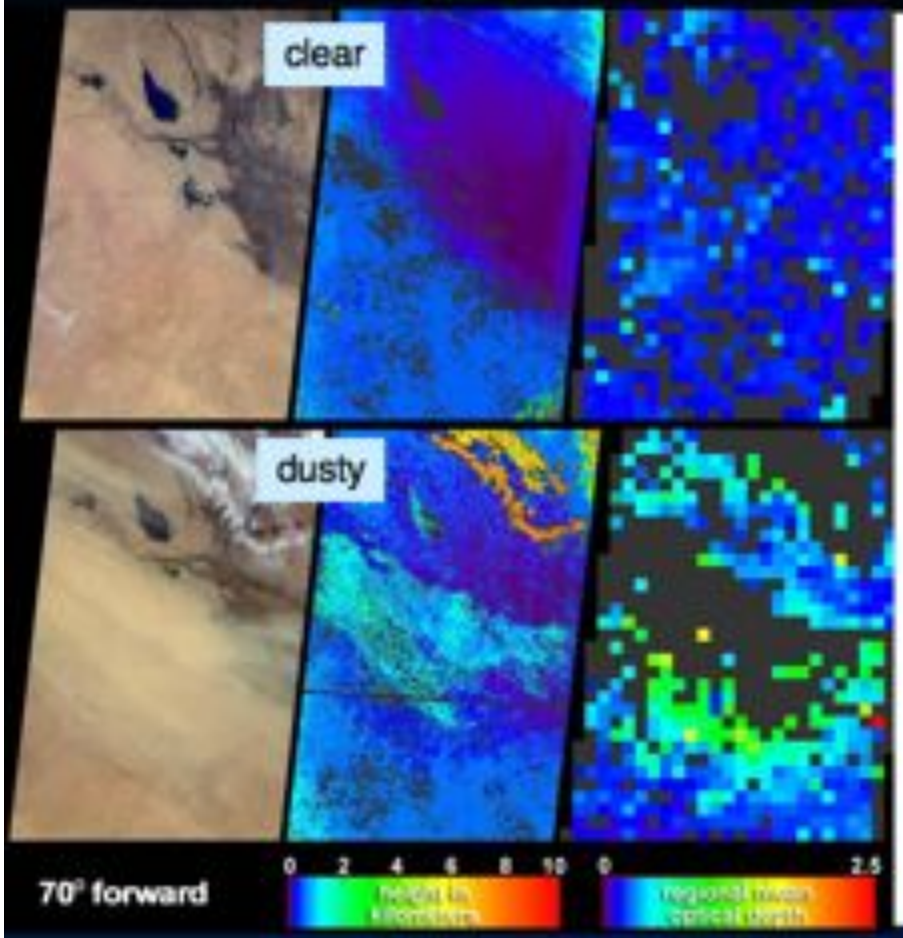

Iraq and Saudi Arabia,
April 2004 (top) and May 2004 (bottom)

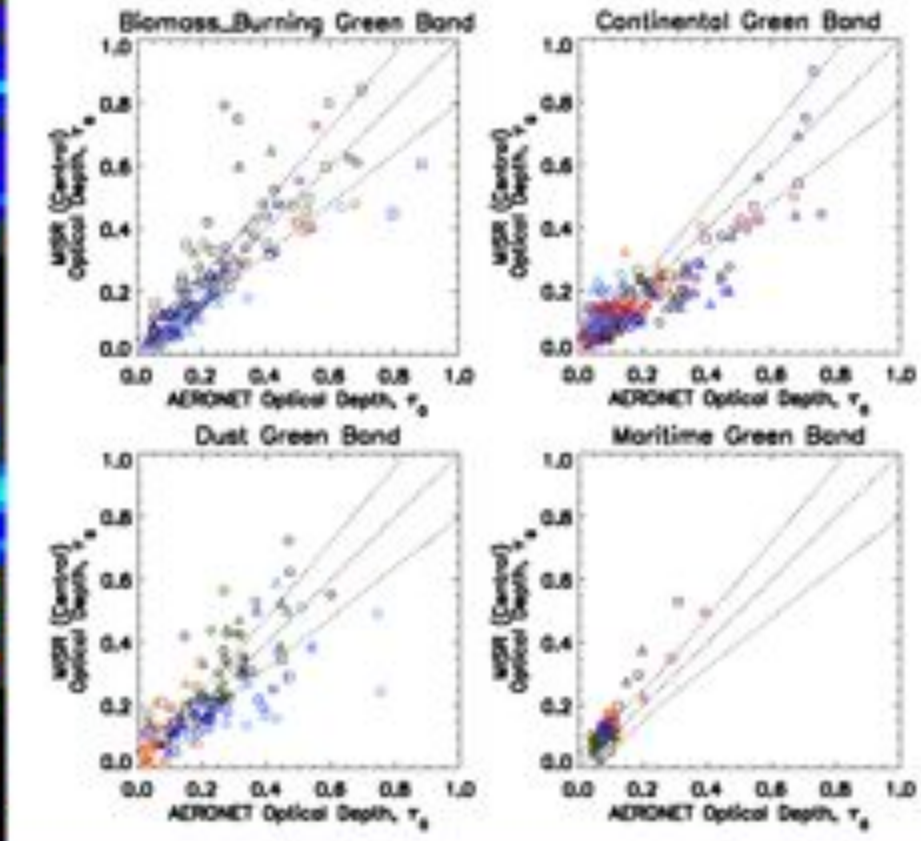

Global optical depth comparisons
With AERONET

A vast pool of tiny particles over India

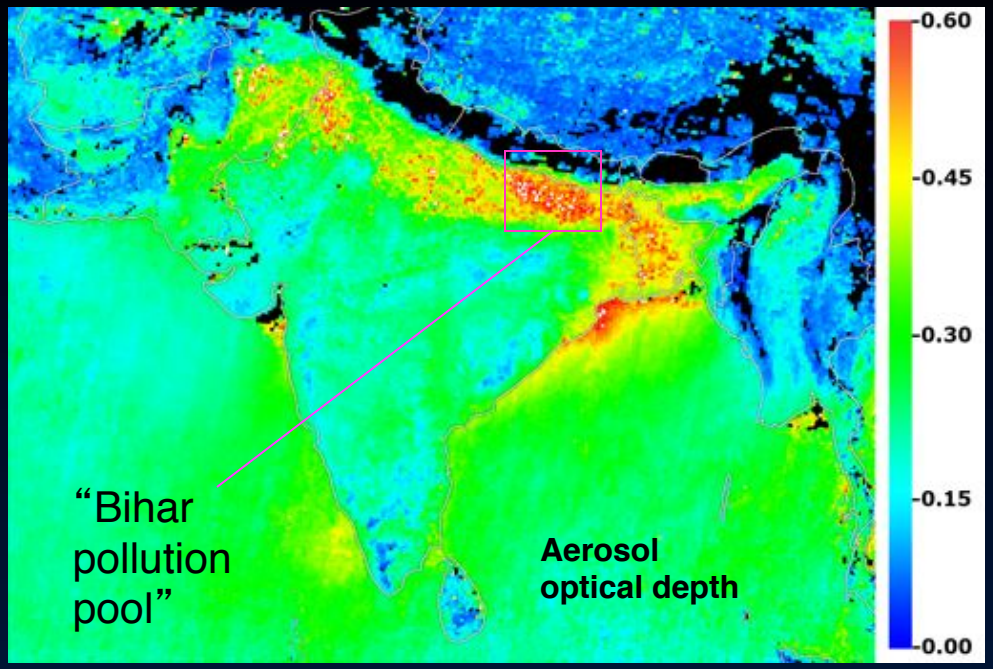

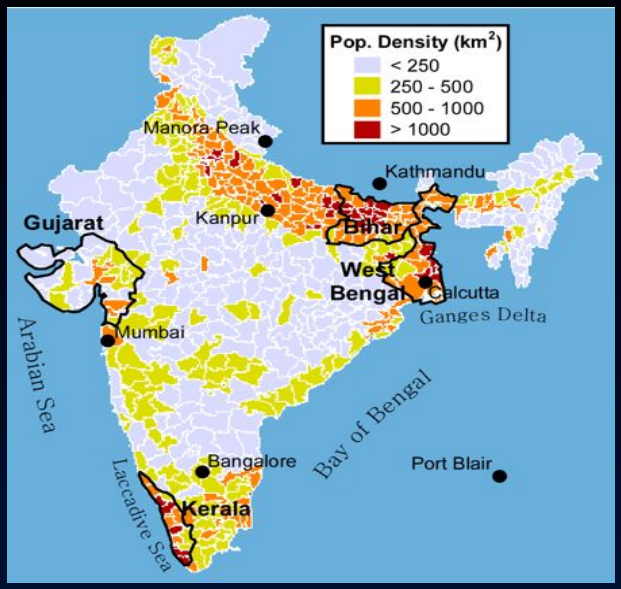

Winter aerosol climatology derived from 4 years of MISR data

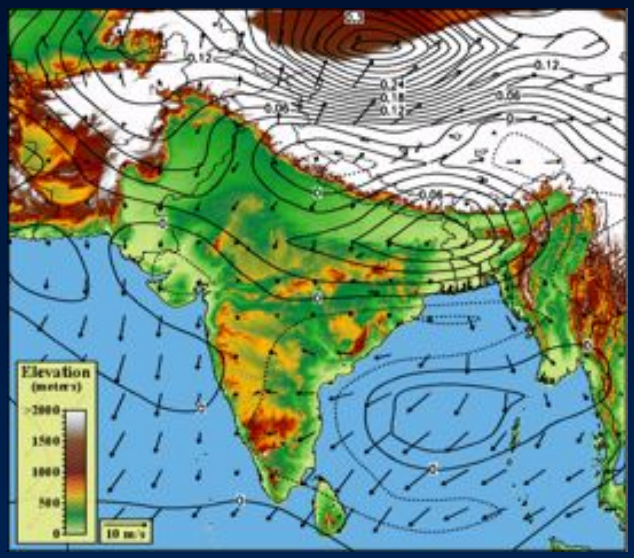

Topography and winds

L. Di Girolamo et al. (2004), GRL

MISR sensitivity to aerosol particle properties

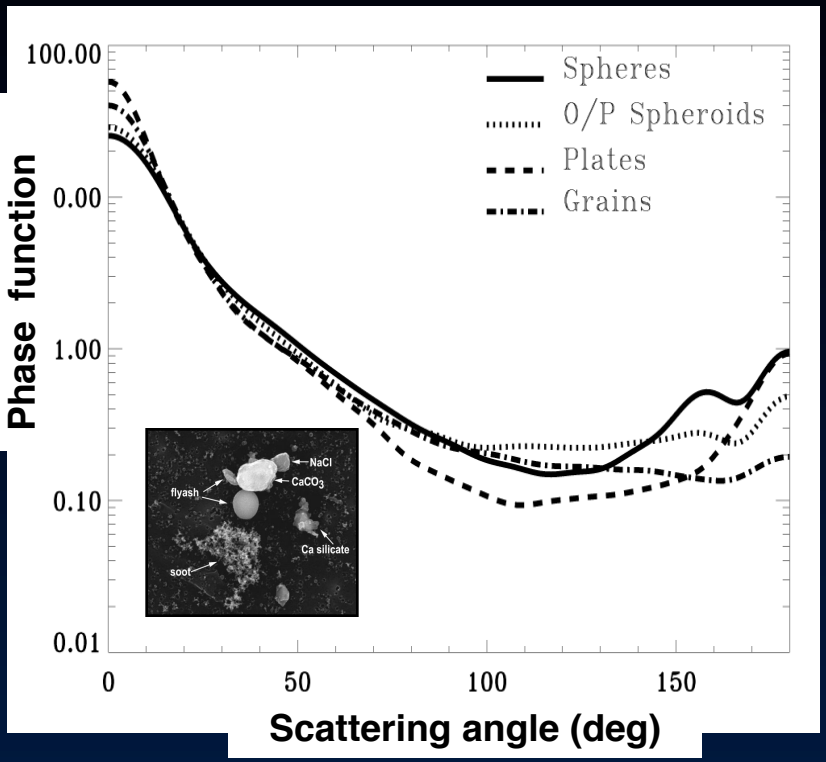

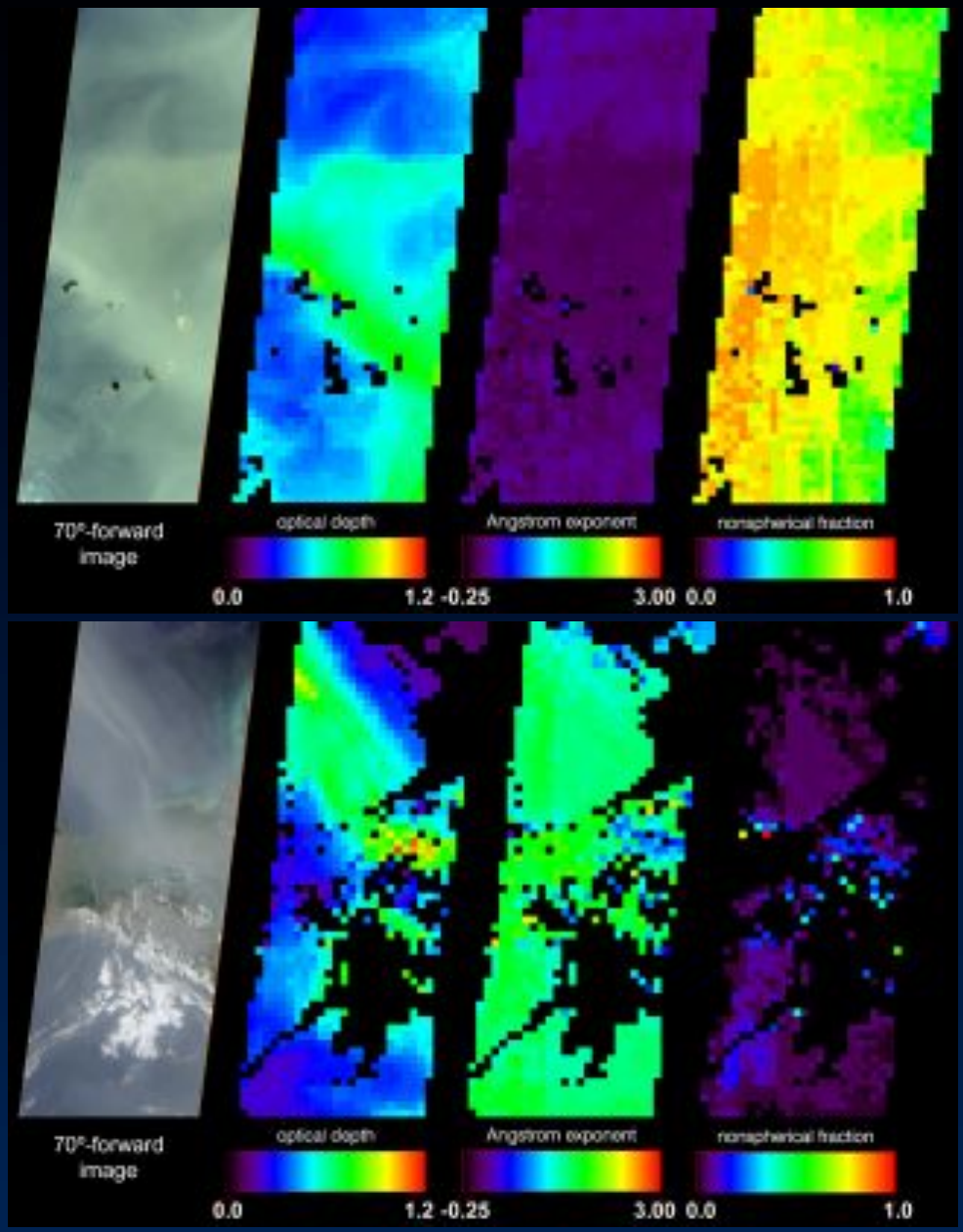

O. Kalashnikova et al. (2005), JGR

Mapping particulate air pollution

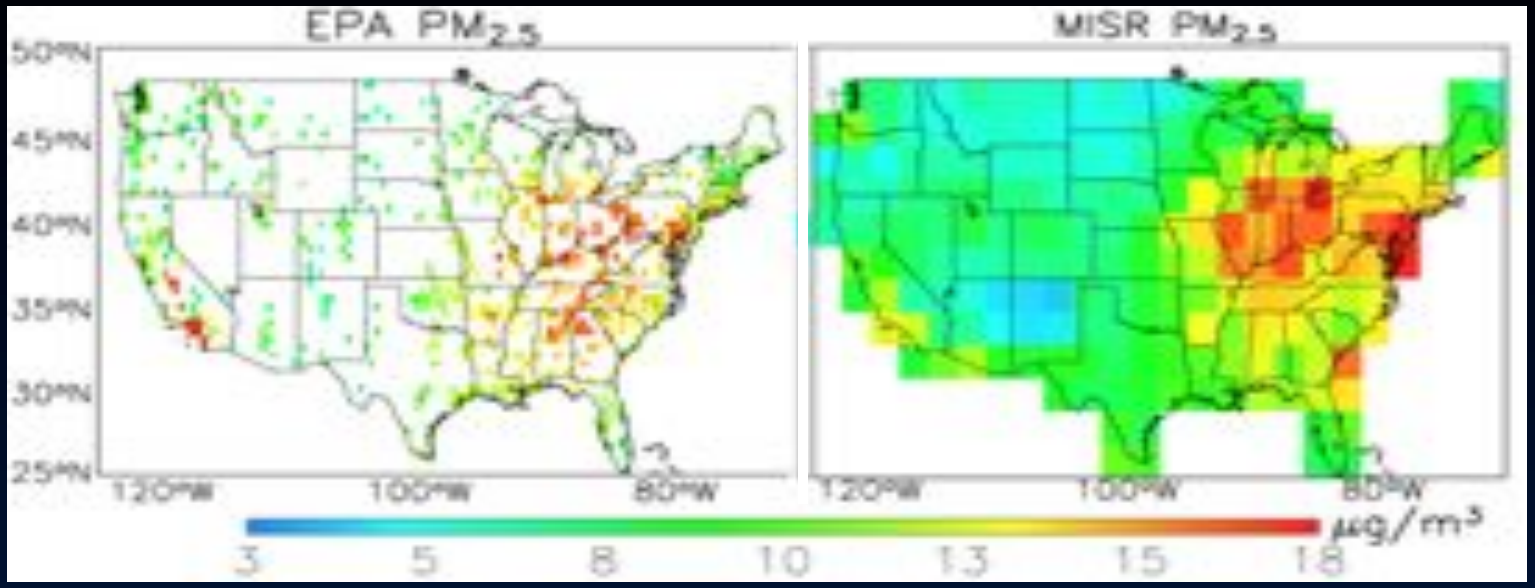

MISR column optical depths are scaled to PM2.5 using a chemical transport model (GEOS-CHEM)

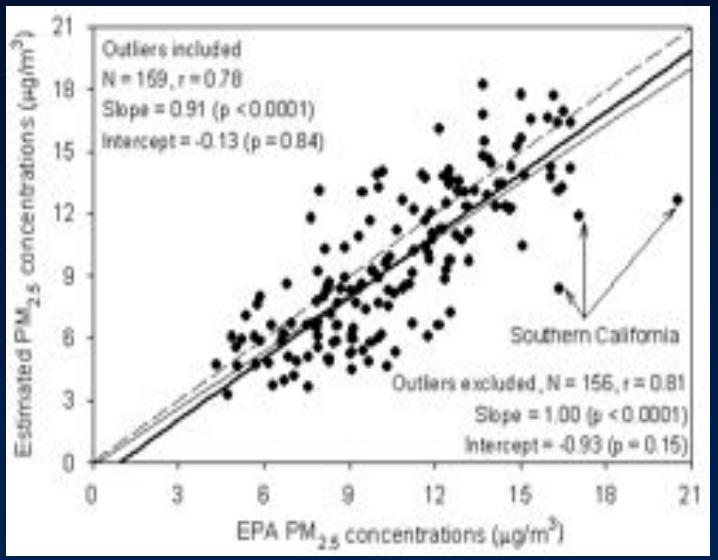

Y. Liu et al. (2005), JGR

L2 Aerosol/Surface Product (MIS05)

Surface parameters

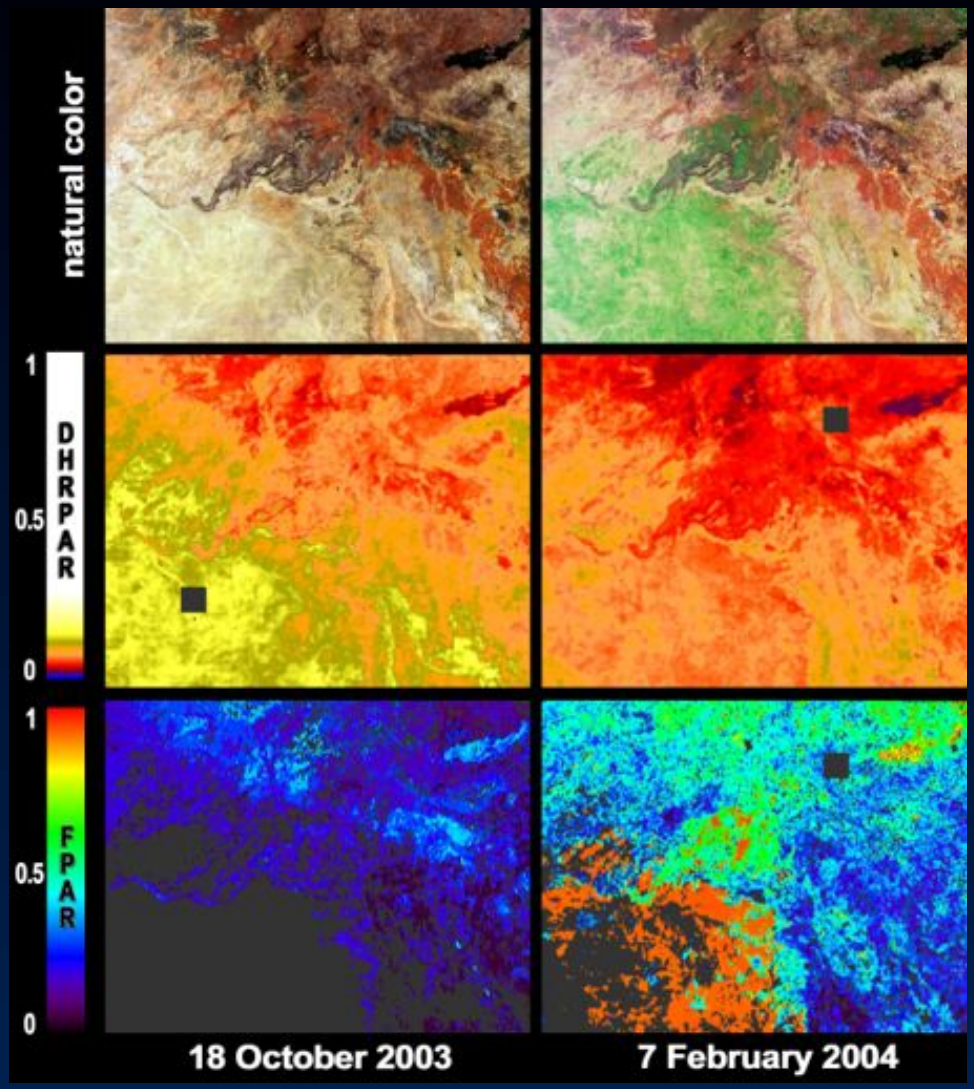

CONTENTS AND ATTRIBUTES

- Radiometric surface parameters (directional reflectances, albedos)

  Derived from single overpass-- no temporal compositing

  Atmospherically corrected

- Vegetation-related quantities (albedo-based surface NDVI, LAI, FPAR)

  LAI-FPAR retrievals are based on 3-D RT models

  Prescribed biome map is not required

- BRF model parameters

Surface greening from summer rains in Northern Queensland

Dependence of bidirectional reflectance on surface vegetation subpixel structure: parametric approach

Structurally homogeneous canopy representation composed of finite-sized scatterers

Parametric models
(e.g., Rahman-Pinty-Verstraete function)
BRF = BRF_0 * Shape term * Asymmetry term
Shape term = $[\mu\mu_0(\mu+\mu_0)]^{k-1}$

Structurally heterogeneous canopy representation composed of clumped ensembles of finite-sized scatterers

Exponent k establishes whether BRF angular signature gets darker off-nadir (bell-shaped, k > 1) or brighter off-nadir (bowl-shaped, k < 1)

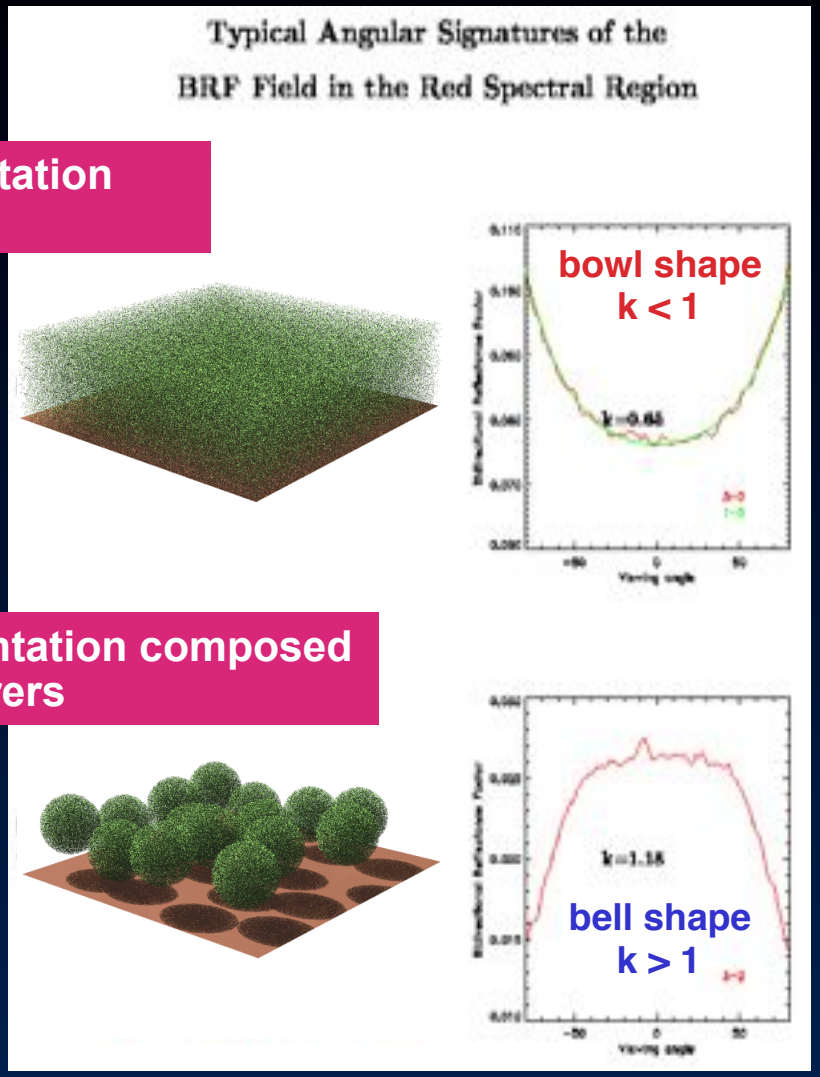

B. Pinty, N. Gobron, J-L. Widlowski, M. Verstraete

Bell and bowl-shaped BRFs

Manitoba and Saskatchewan, 17 April 2001

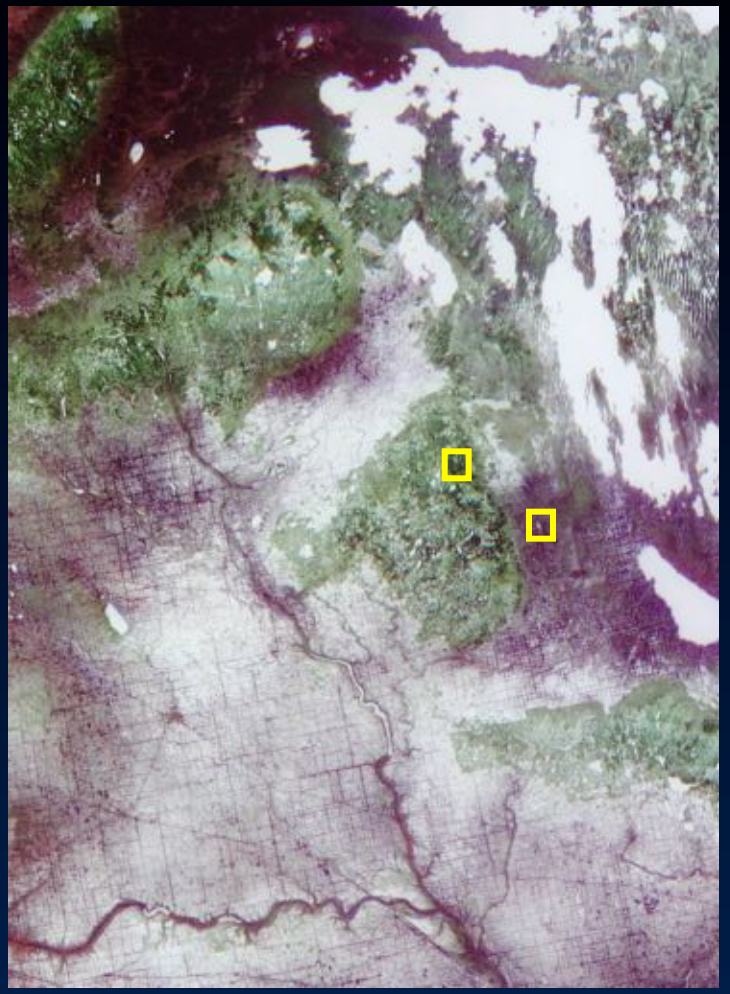

Nadir false-color composite:
RGB = near-IR, red, green

Multi-angle red band composite:
RGB = 60° backward, nadir, 60° forward

Bidirectional reflectances of surface vegetation as observed by MISR

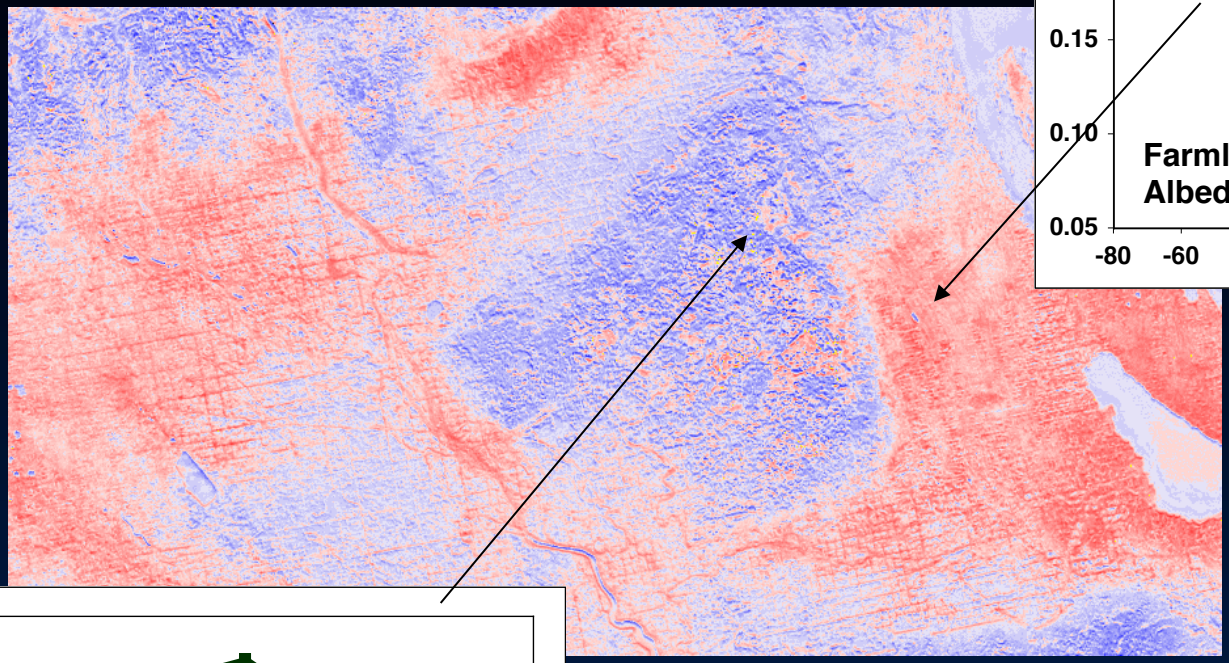

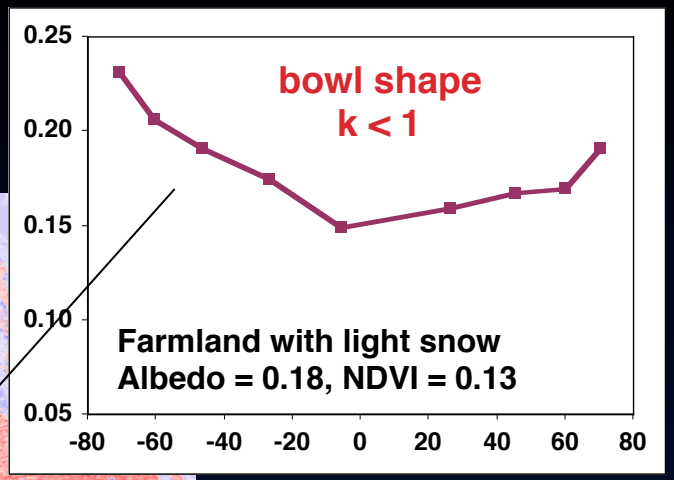

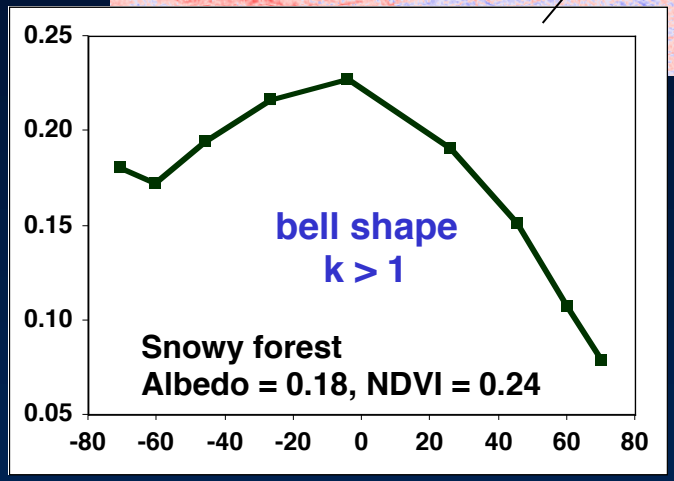

Manitoba and Saskatchewan, 17 April 2001

k-parameter

B. Pinty, N. Gobron, J-L. Widlowski, M. Verstraete

Relationship between surface vegetation bidirectional reflectance and canopy structure

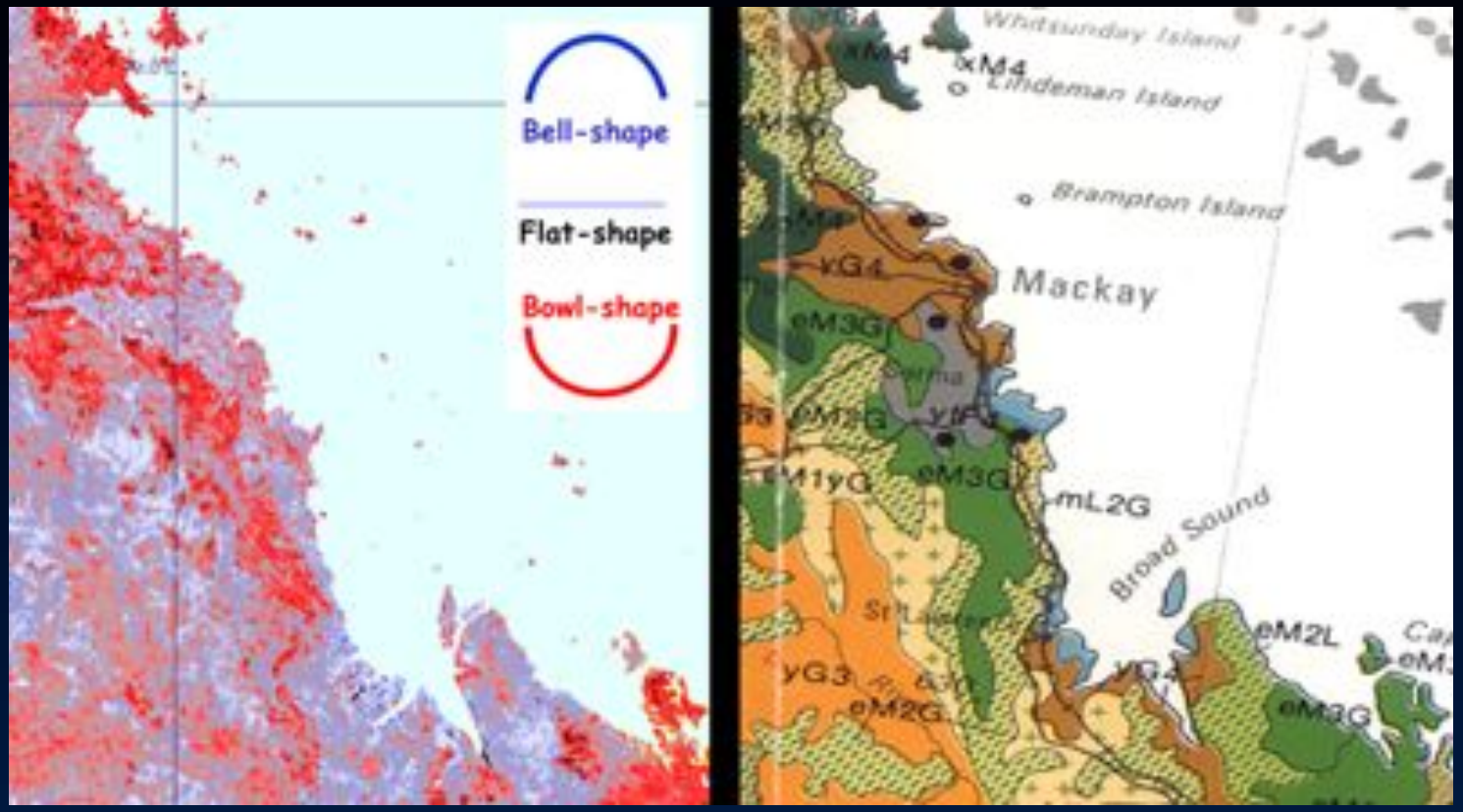

Australian Surveying & Land Information Group

Bowl-shaped BRF: Sparse vegetation and dense, closed canopies

Bell-shaped BRF: Tree crowns of medium-high density against bright background

B. Pinty (JRC), N. Gobron (JRC), J-L. Widlowski (JRC), M. Verstraete (JRC)

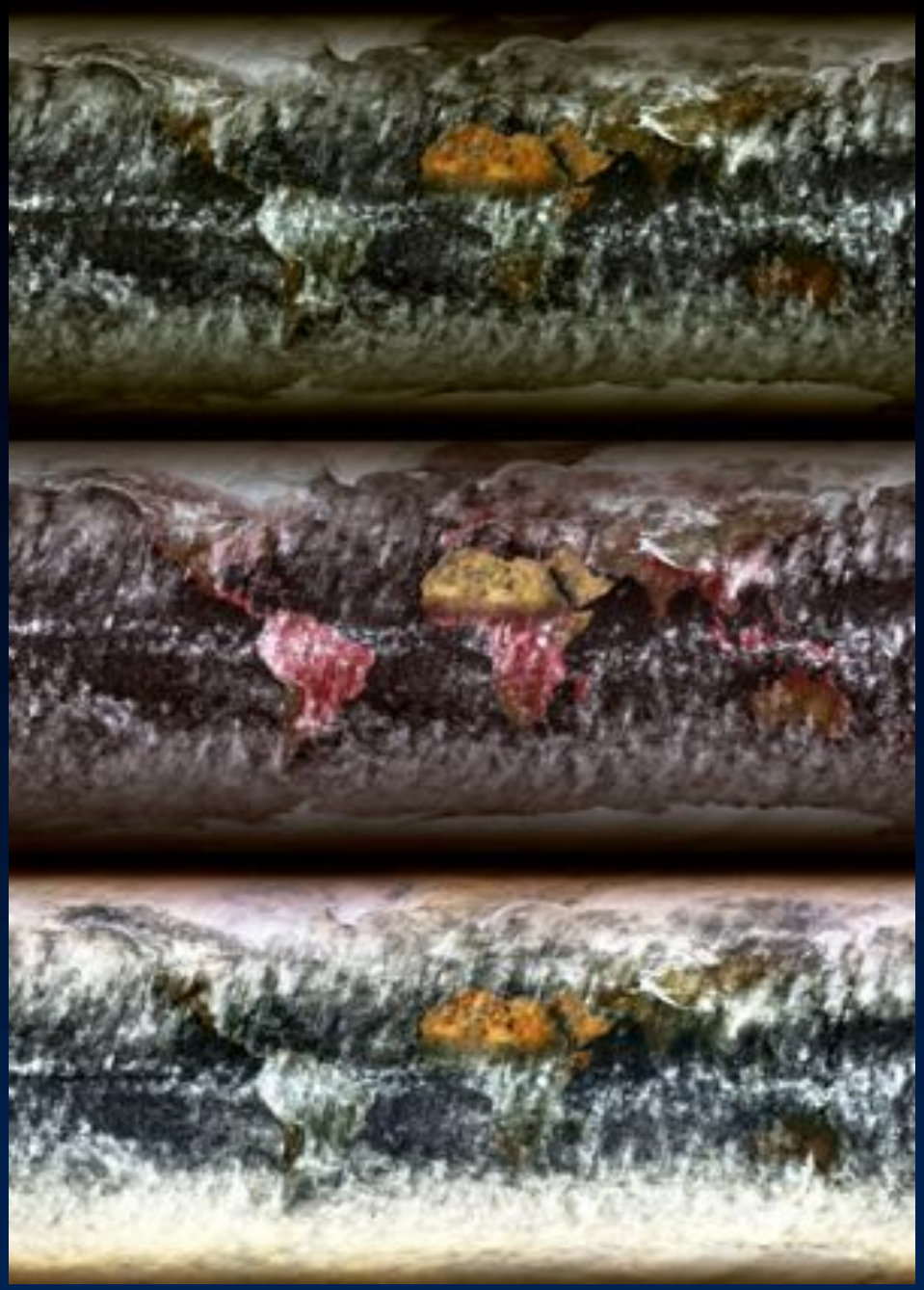

L3 Gridded Radiances (MIS06)

Means, variances, and covariances

Nadir red, green, blue

Nadir near-infrared, red, green

March 2002

70° forward: red, green, blue (N. hemisphere)
70° backward: red, green, blue (S. hemisphere)

L3 Gridded Aerosol (MIS08)

Global optical depths

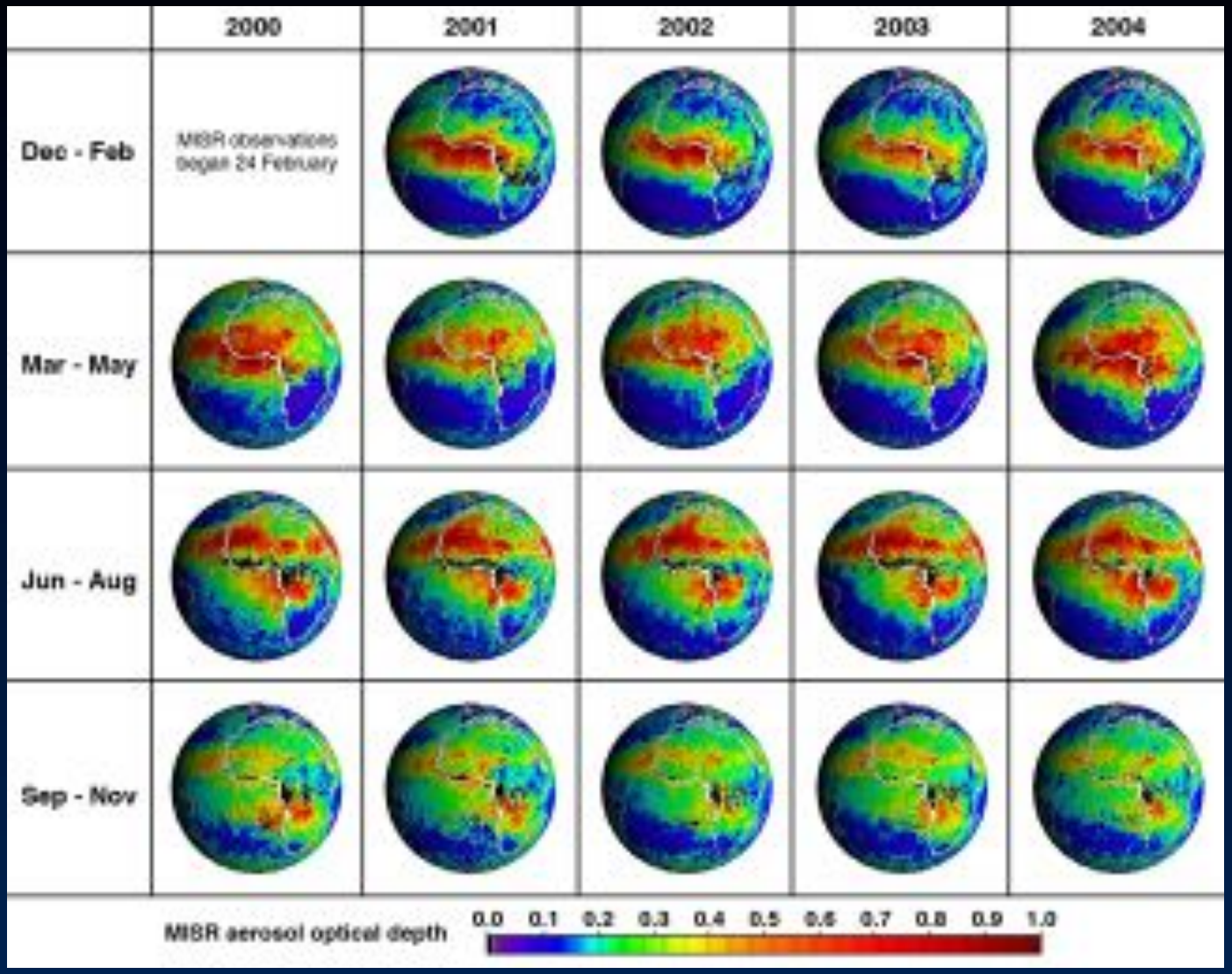

L3 Gridded Surface (MIS09)

Radiative and biogeophysical parameters

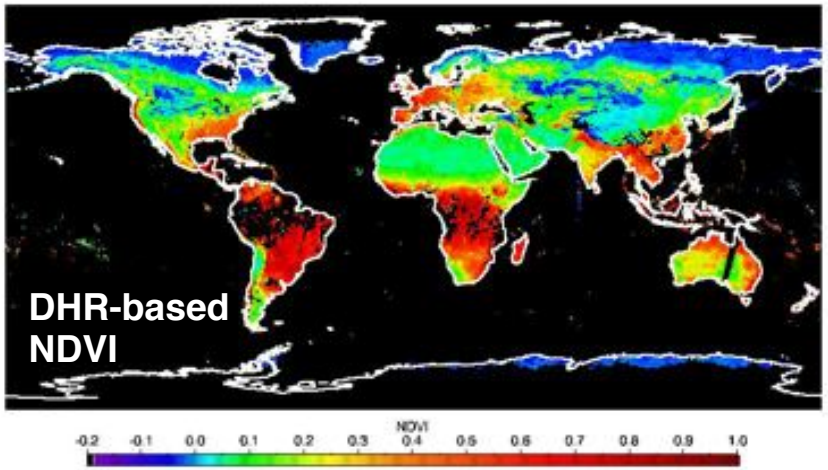

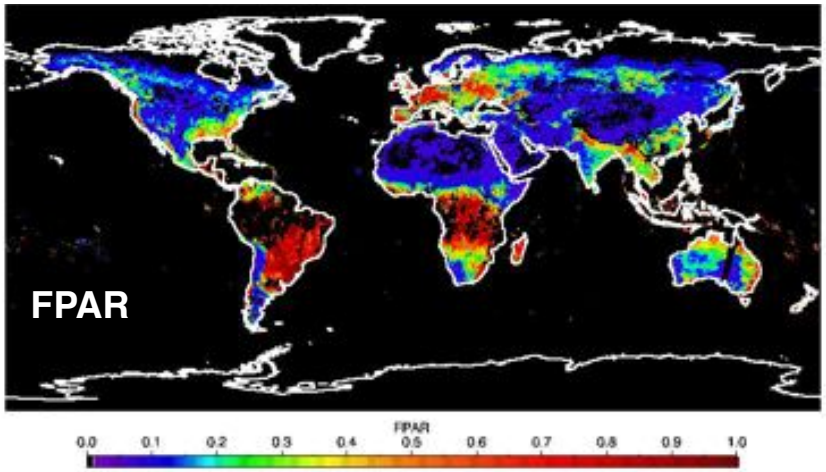

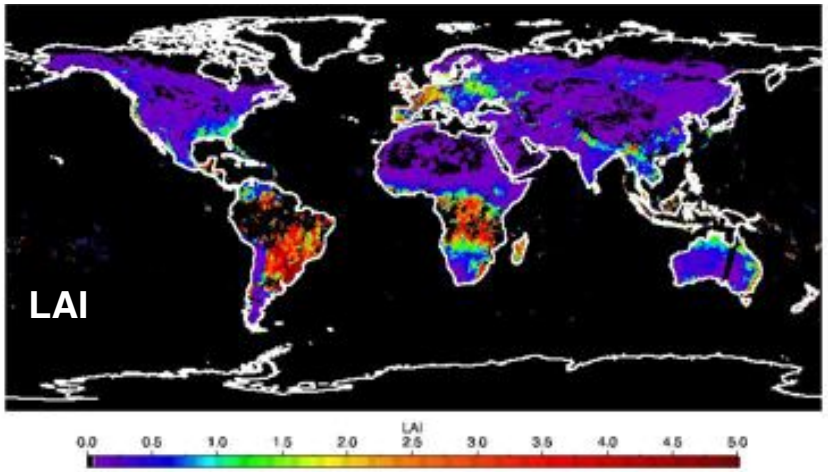

Additional products you might need

Ancillary Geographic Product

--contains latitudes, longitudes, elevations, scene classifiers for each 1.1-km pixel on the Space Oblique Mercator grid

Aerosol Climatology Product

--Aerosol Physical and Optical Properties (APOP) contains characteristics of the component particles used in the aerosol retrievals

--Mixture file contains characteristics of the particle mixtures used

Data quality and maturity levels

Terra data products are given the following maturity classifications:

Beta: Minimally validated. Early release to enable users to gain familiarity with data formats and parameters. May contain significant errors.

Provisional: Partially validated. Improvements are continuing. Useful for exploratory studies.

Validated: Uncertainties are well defined, and suitable for systematic studies.

Mapping of data product maturity to version numbers found at:
eosweb.larc.nasa.gov/PRODOCS/misr/Version/

Be sure to read the quality statements!
eosweb.larc.nasa.gov/PRODOCS/misr/Quality_Summaries/misr_qual_stmts.html

Where to get help and information

LaRC DAAC User Services
larc@eos.nasa.gov

Langley Atmospheric Sciences Data Center DAAC
http://eosweb.larc.nasa.gov

MISR home page
http://www-misr.jpl.nasa.gov

We welcome your feedback and questions!
"Ask MISR" feature on the MISR web site